"Japan-Russia Workshop on Supercomputer Modelling, Instability and Turbulence in Fluid Dynamics (JR SMIT2015)" March 2015, Moscow

Clustering and Entropy Growth of Quasi-geostrophic Point Vortices under Periodic Boundary Conditions

Takeshi Miyazaki with students

The University of Electro-Communications (UEC)
Email : miyazaki@mce.uec.ac.jp
1-5-1 Chofugaoka, Chofu, Tokyo 182-8585, Japan

Outline

Background

The relevance of vortices in Geophysical flows

Quasi-geostrophic Approximation

Hierarchy of vortex based models of geostrophic turbulence

Statistical Mechanics of QG Point Vortices

Mono-disperse system in an infinite domain (briefly)

Bi-disperse system of mixed sign under periodic conditions

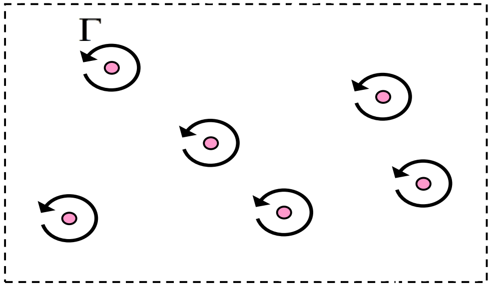

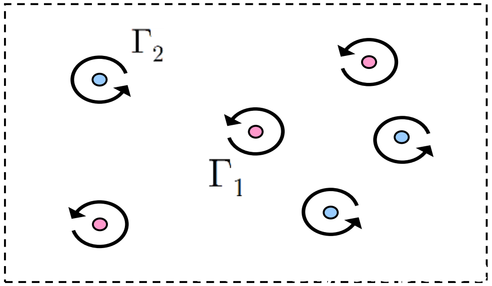

- Simulation results → Transient behavior and Equilibrium state
- Comparison with the Maximum entropy theory
- Stability of the equilibrium state

Background-1

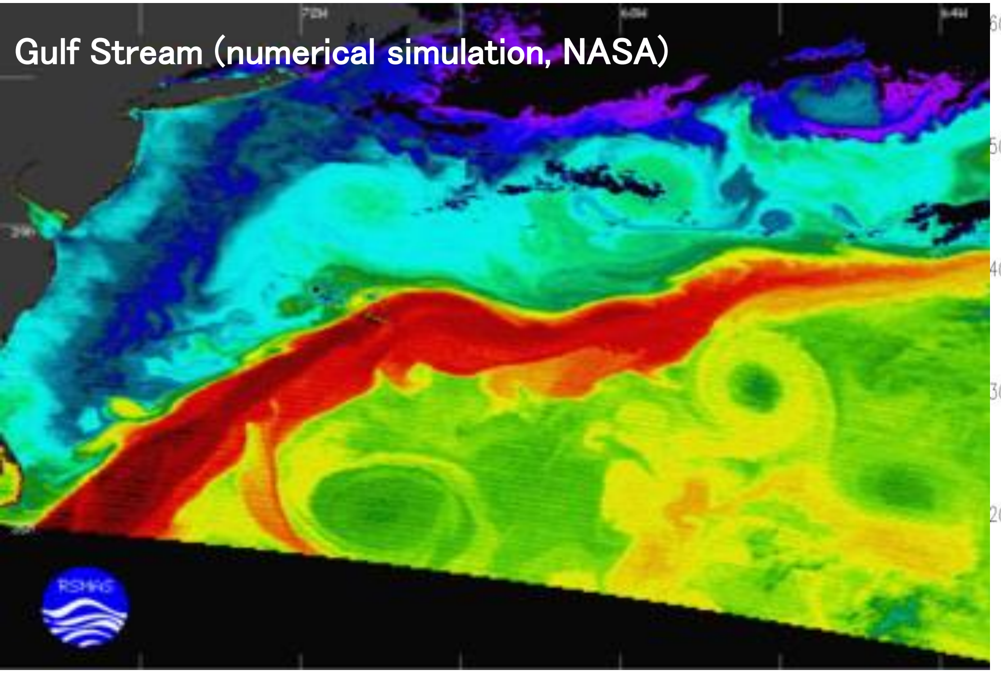
Gulf Stream (numerical simulation, NASA)

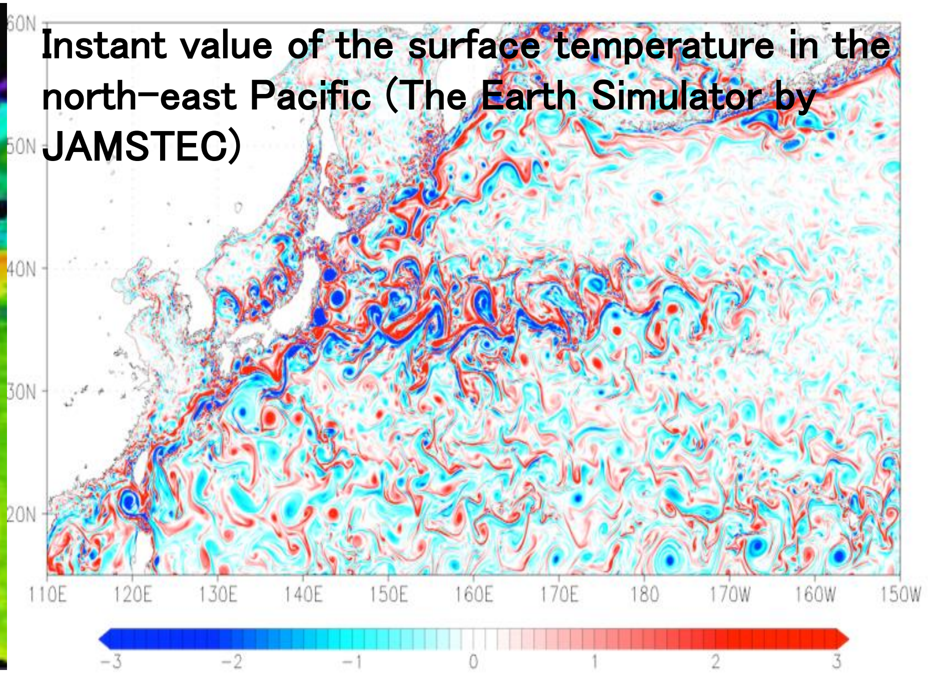

Instant value of the surface temperature in the north-east Pacific (The Earth Simulator by JAMSTEC)

Geophysical flows ···

Vertical motion is suppressed due to the Coriolis force and stable stratification.

> In a rotating stratified fluid, the interactions of isolated coherent vortices dominate the turbulence dynamics.

Background-2: Theoretical Approach

Two-dimensional point vortex systems

lowest order approximation of geophysical flows

■ **Many statistical studies**

have been made on purely 2D flows.

Statistical mechanics

☑ L. Onsager (1949),
negative temperature

☑ D. Montgomery and G. Joyce (1974),
canonical ensemble

☑ Y. B. Pointin and T. S. Lundgren (1976),
micro canonical ensemble

☑ Yatsuyanagi *et al*. (2005),
very large numerical simulation (N = 6724)

The actual geophysical flows are 3D.

■ The fluid motions are almost confined within a horizontal plane.

■ Different motions are allowed on different horizontal planes.

'Quasi-geostrophic approximation'

(next order approximation)

⇒The QG-approximation confines the motion in different horizontal planes.

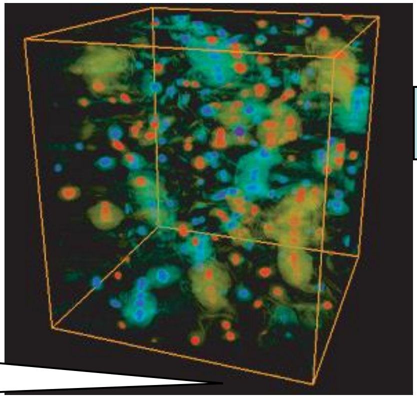

J. C. McWilliams *et al*. (1994)
Coherent vortex structures in QG turbulence

2-layer QG point vortex system (2001)
by Mark T. DiBattista and Andrew J. Majda

Vortex models

Point vortex	*N* degrees of freedom
Spheroidal vortex	2*N* degrees of freedom — **Miyazaki *et al.* (2005)**
Ellipsoidal vortex	3*N* degrees of freedom — **Li *et al.* (2006)**

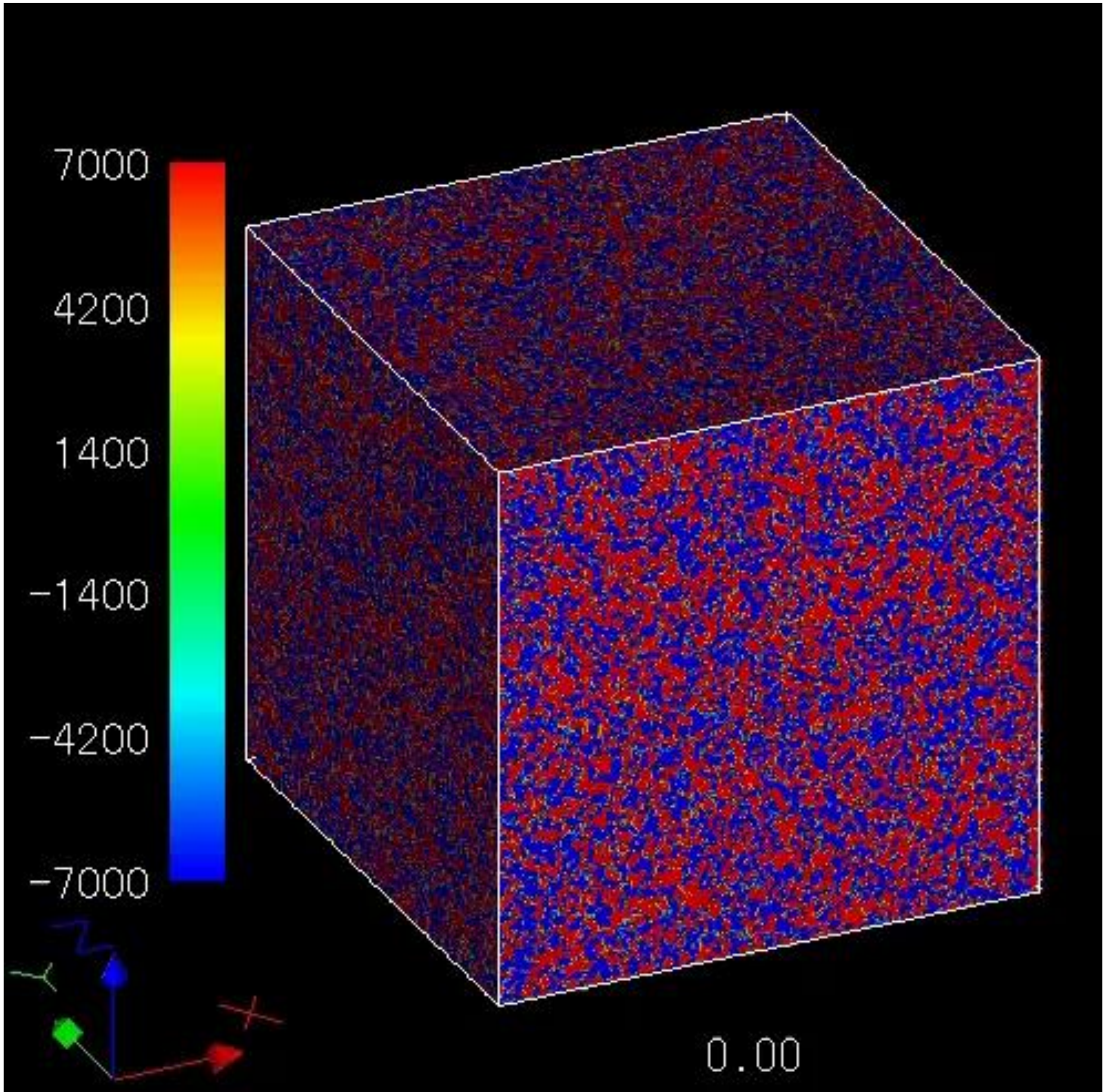
7000
4200
1400
-1400
-4200
-7000
0.00

Objective

Statistical Mechanics of QG Point Vortices

Numerical Computations using

Special Purpose Computers

Theoretical Studies based on

Maximum Entropy Theory

Quick review of

Mono-disperse System in an Infinite Domain

Mainly

Bi-disperse System in a Periodic Box

Quasi-geostrophic Approximation

2D Fluid motion (Ψ : stream function)

$$u = \frac{\partial \Psi}{\partial y}, \quad v = -\frac{\partial \Psi}{\partial x}, \quad w = O\left(\frac{f_0}{N}\right)$$

$N \fallingdotseq 1.16 \times 10^{-2}\,\mathrm{s}^{-1}$, $f_0 \sim 1/(24[\mathrm{h}])$

N : Brunt-Vaisala frequency

f_0 : Coriolis parameter ($f_0 = 2\Omega \sin\theta$ by at latitude θ)

Time-evolution under the quasi-geostrophic approximation

$$\left(\frac{\partial}{\partial t} + \frac{\partial \Psi}{\partial y}\frac{\partial}{\partial x} - \frac{\partial \Psi}{\partial x}\frac{\partial}{\partial y}\right) q = 0$$

Potential vorticity

$$q = -\Delta \Psi = -\left(\frac{\partial^2}{\partial x^2} + \frac{\partial^2}{\partial y^2} + \frac{\partial^2}{\partial z^2}\right)\Psi$$

Point vortex systems $\hat{\Gamma}_i$: strength, $\boldsymbol{R}_i$: location

$$q = \sum_{i=1}^{N} \hat{\Gamma}_i \delta(\boldsymbol{r} - \boldsymbol{R}_i), \quad \boldsymbol{r} = (x, y, z)$$

Assuming δ-function like concentration at N points, each vortex is advected by the flow field induced by other vortices.

Equations of Motion for Quasi-geostrophic Point Vortices

Canonical Variables : X, Y

Hamiltonian of QG *N* point vortex system (invariant)

$$H = \sum_{(i,j)}^{N} H_{mij}, \quad H_{mij} = \frac{\hat{\Gamma}_i \hat{\Gamma}_j}{4\pi |\boldsymbol{R}_i - \boldsymbol{R}_j|}$$

interaction energy

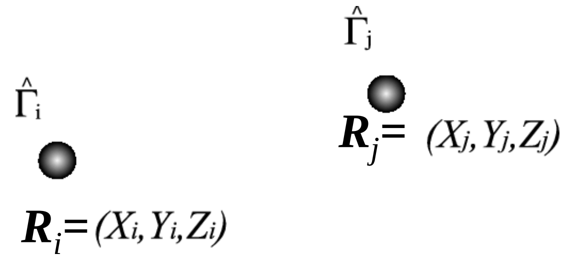

Canonical equations of motion for the ***i*−**th vortex

$$\frac{\mathrm{d}X_i}{\mathrm{d}t} = \frac{1}{\hat{\Gamma}_i}\frac{\partial H}{\partial Y_i}, \qquad \frac{\mathrm{d}Y_i}{\mathrm{d}t} = -\frac{1}{\hat{\Gamma}_i}\frac{\partial H}{\partial X_i}$$

Computation on Special Purpose Computers: MDGRAPE-3, -DR, GRAPE9

Time Integration with LSODE (6 significant digits)

t : dimensionless time (in units of the inverse potential vorticity)

□ MDGRAPE-3, MDGRAPE-DR, GRAPE9

© http://mdgrape.gsc.riken.jp

RIKEN

Specifications

Number of MFGRAPE-3 Chip : 2

Performance : 330 Gflops (peak)

Host Interface : PCI-X 64bit/100MHz

Power Consumption : 40 W

Maximum Entropy Theory for Mono-disperse System

Conserved quantities

Vertical distribution

$$P(z) = \iint F(\boldsymbol{r}) dxdy \quad \left(\int_{z_1}^{z_2} P(z) dz = 1 \right)$$

Angular momentum

$$\hat{I} = \iiint (x^2 + y^2) F(\boldsymbol{r}) d^3\boldsymbol{r} = 1$$

Energy

$$\frac{8\pi H}{\hat{N}^2} = \iiiint\!\!\iint \frac{F(\boldsymbol{r})F(\boldsymbol{r}')}{|\boldsymbol{r} - \boldsymbol{r}'|} d^3\boldsymbol{r} d^3\boldsymbol{r}'$$

Shannon entropy

$$\log \hat{Z} = -\hat{N} \iiint F(\boldsymbol{r}) \log F(\boldsymbol{r}) d^3\boldsymbol{r}$$

Lagrange's undetermined multipliers

Numerical iteration

$$\log F(\boldsymbol{r}) + 1 + \alpha(z) + \beta(x^2 + y^2) + \frac{\gamma}{4\pi} \iiint \frac{F(\boldsymbol{r}')}{|\boldsymbol{r} - \boldsymbol{r}'|} d^3\boldsymbol{r}' = 0$$

$\gamma = 0$

"0-inverse-temperature"

$$F^{zit}(r, z) = \frac{P(z)}{\pi} e^{-r^2}$$

Two-dimensional point vortices by Kida (J. P. S. J., 39(5) (1975), pp.1395-1404)

Equilibrium States in an Infinite Domain

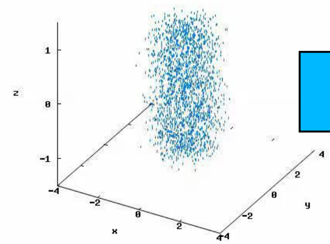

Potential vorticity

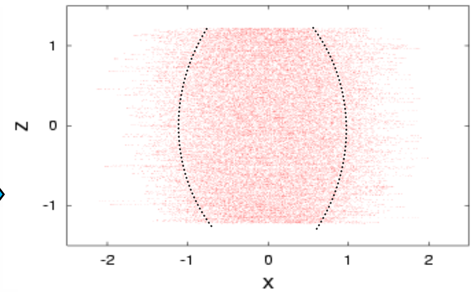

Positive

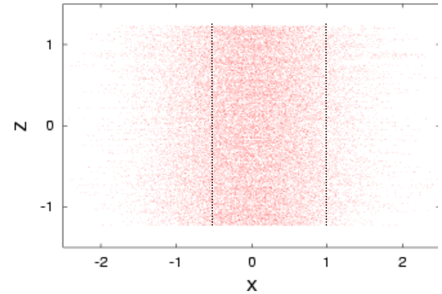

Zero inverse temperature

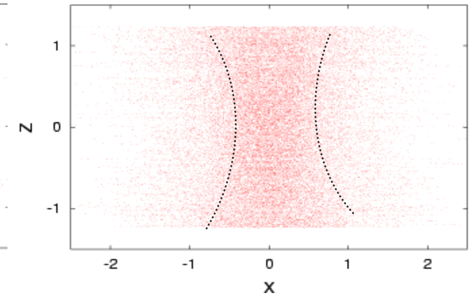

Negative

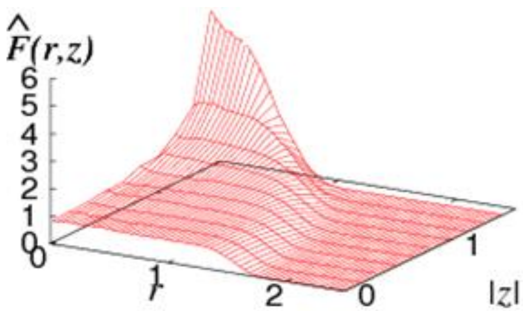

Positive

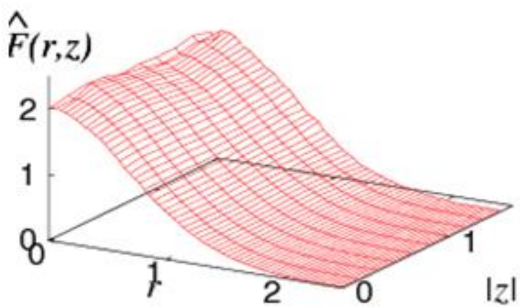

Zero inverse

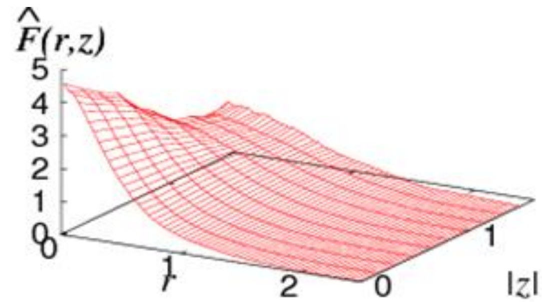

Negative

Maximum entropy states

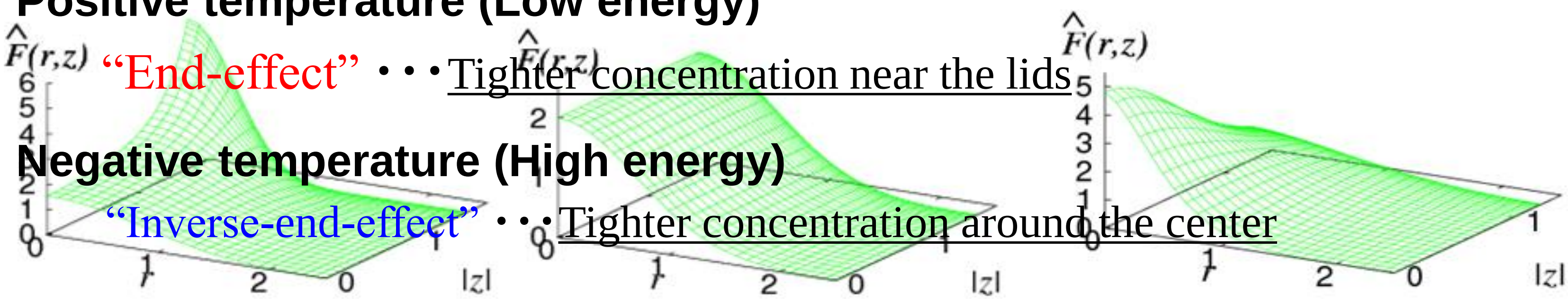

Positive temperature (Low energy)

"End-effect" • • • Tighter concentration near the lids

Negative temperature (High energy)

"Inverse-end-effect" • • • Tighter concentration around the center

Mono-disperse System in an Infinite Domain

Quick summary

- **Mono-disperse system of same sign:**
  the radial distribution changes with the energy level:
  Positive, zero-inverse and negative temperature states

- **Numerical results are consistent with the theoretical results of the Maximum entropy theory**

- **It takes quite long to obtain a well developed numerical equilibrium**

References ;

- **S. Hoshi and T. Miyazaki: Fluid Dynamics Research (2008)**
- **T. Miyazaki, T. Sato, H. Kimura and N. Takahashi: Geophysical and Astrophysical Fluid Dynamics (2011)**
- **T. Miyazaki, T. Sato and N. Takahashi: Phys. Fluids (2012)**

Bi-disperse system of mixed sign: $\Gamma_1 = -\Gamma_2$

QG Bi-disperse Point Vortices : $\Gamma_1 = -\Gamma_2$ $N = N_+ = N_-$

- Geophysical flows ･･･ Poly-disperse, Mixed sign, ･･･

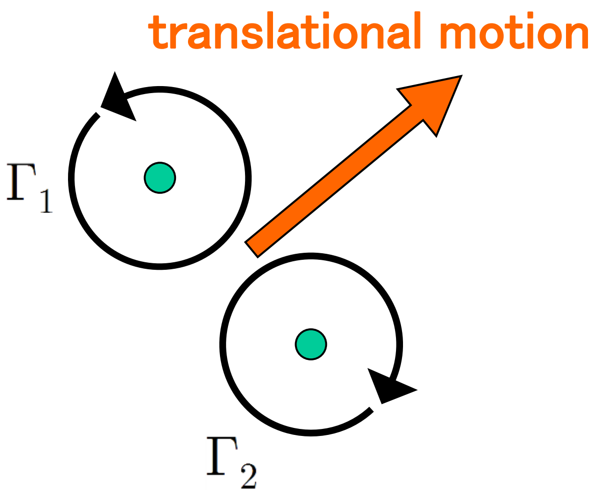

Counter-rotating : $\Gamma_1 = -\Gamma_2$

Problem

Because the vortices diffuse towards infinity,
They drift outside the secure calculation area
of the MDGRAPE-3, GRAPE-DR and GRAPE9.

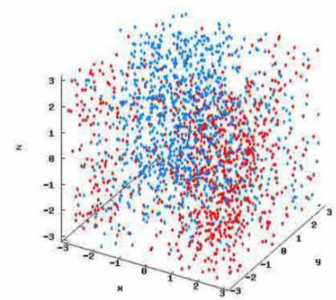

Red : plus sign
Blue : minus sign

We have to calculate under periodic boundary conditions

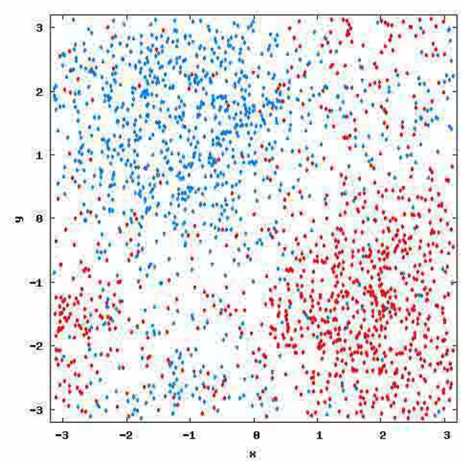

"Ewald sum", as frequently used in Molecular Dynamics

Replacement of real-space summation with equivalent summation in Fourier space under the periodic boundary conditions

Numerical Results: Small System (*N*=1000)

- **Initial structure : Two-dimensional**

E=6.413×10^-3

X-Y

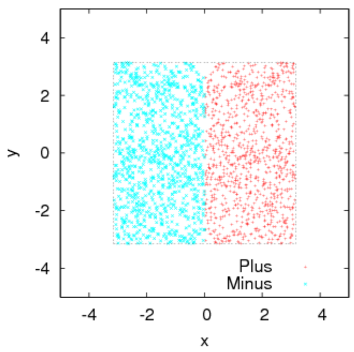

X-Z

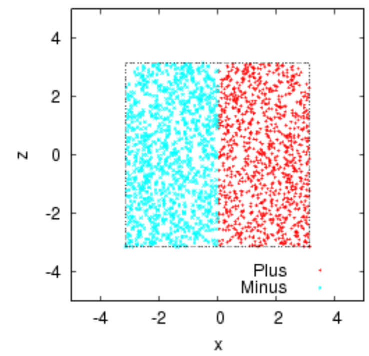

E=2.424×10^-3

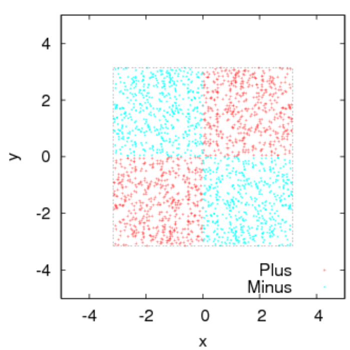

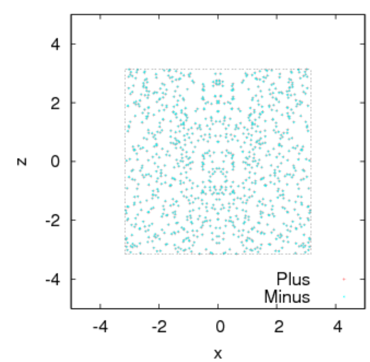

Plus $N_{\pm} = 1000$ **Minus**

Time-evolution

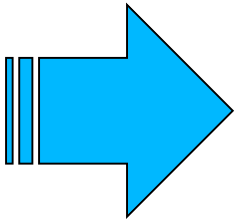

Equilibrium

X-Y

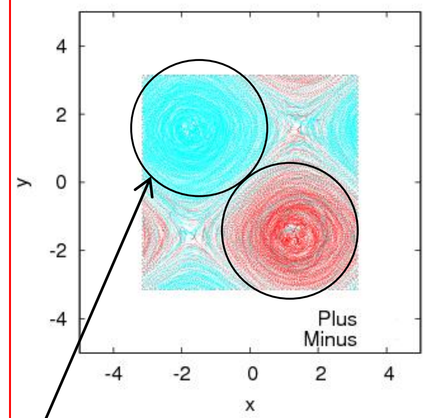

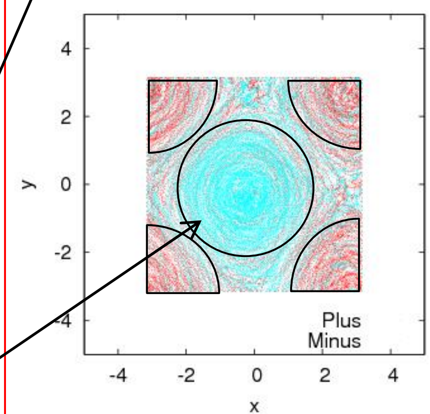

Clustering $P_{\pm}(z) = 1/2\pi$

- Does the energy determine the equilibrium state uniquely ?
- Are all equilibrium states two-dimensional ?

Numerical Results: Small System (N=1000)

☐ Three-dimensional Initial Distribution

Time-evolution

$E=2.714\times 10^{-3}$

X-Y

X-Z

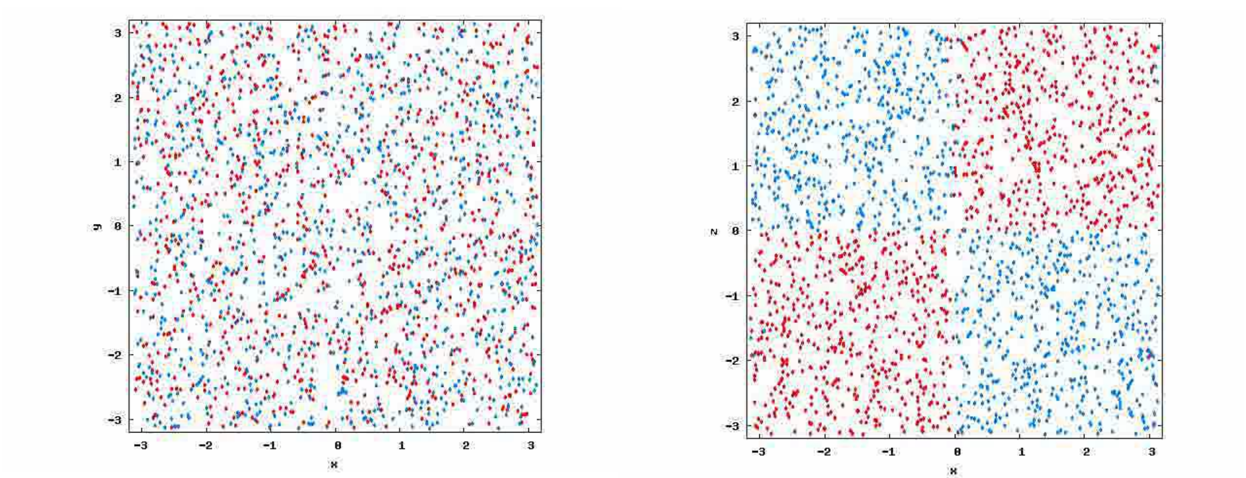

X-Y

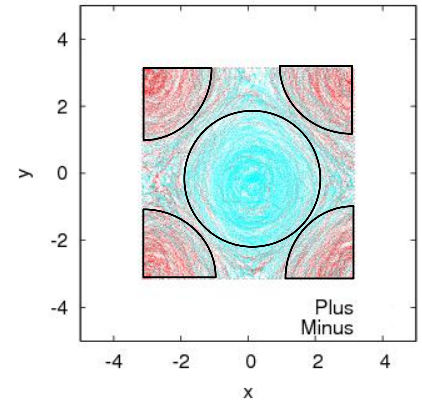

- Transition from three-dimensional to two-dimensional structure !
- Is there a unique equilibrium state at a specified energy level ?
- How does the system approach the equilibrium state ?

Transient Behavior: Larger Systems

$$L_x : L_y : L_z = 2\pi : 2\pi : 2\pi$$

Case A: **3D dipole**

$E = 10.01 \times 10^{-3}$
$N_+ = 4000$
$N_- = 4000$
$\hat{\Gamma}_\pm = 0.062$

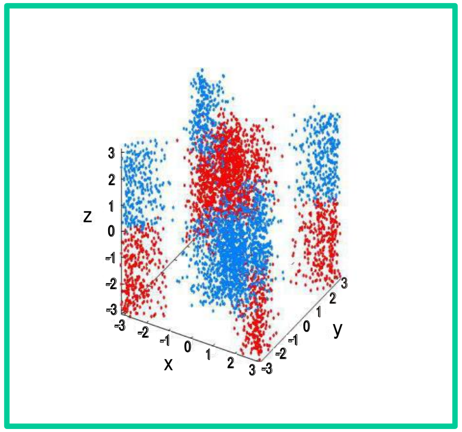

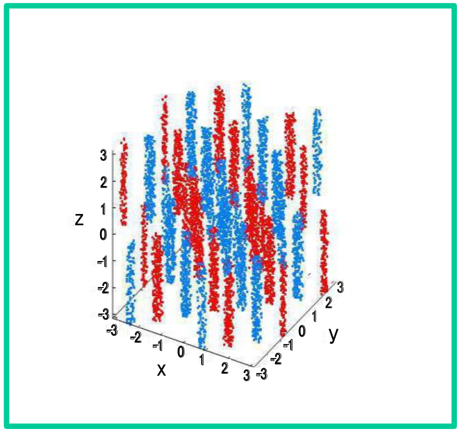

Case B: **Checkerboard**

$E = 4.428 \times 10^{-3}$
$N_+ = 4000$
$N_- = 4000$
$\hat{\Gamma}_\pm = 0.062$

Case C: **16 pillars**

$E = 2.426 \times 10^{-3}$
$N_+ = 4000$
$N_- = 4000$
$\hat{\Gamma}_\pm = 0.062$

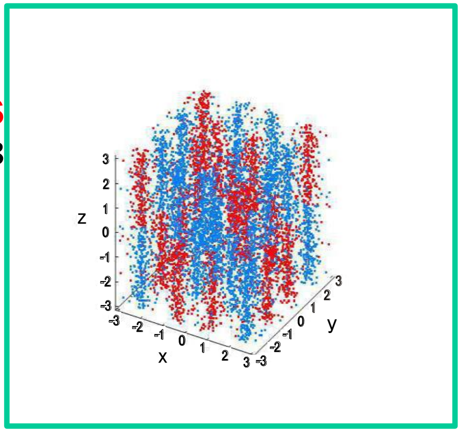

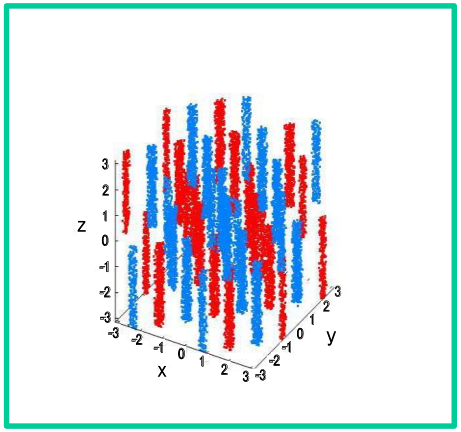

Case D: **Checkerboard**

$E = 4.536 \times 10^{-3}$
$N_+ = 8000$
$N_- = 8000$
$\hat{\Gamma}_\pm = 0.031$

End States of Larger Computations

$L_{x,y,z} = 2\pi$

$N = 4000$

Plus $N_+ = 4000$

Minus $N_- = 4000$

Strength

$\hat{\Gamma}_{\pm} = \pm 0.062$

Dipole Pair Moves

Not in Equilibrium

Initial

Case C

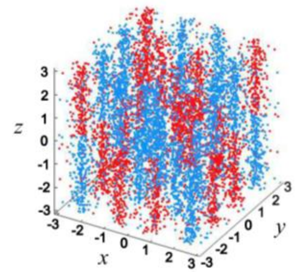

$E = 2.426 \times 10^{-3}$

$t = 150$

Case B

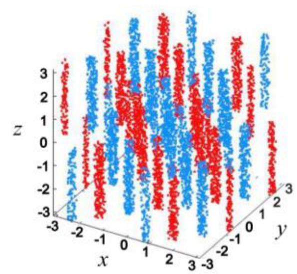

$E = 4.428 \times 10^{-3}$

$t = 158$

Case A

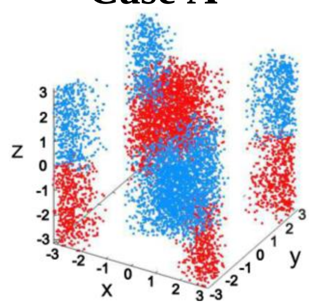

$E = 10.01 \times 10^{-3}$

$t = 180$

End States: sn-sn dipole？

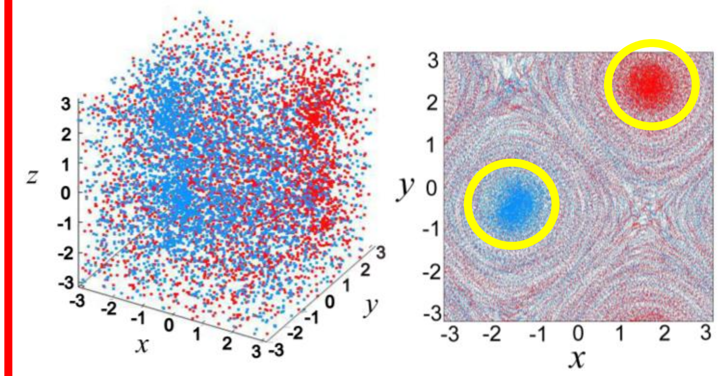

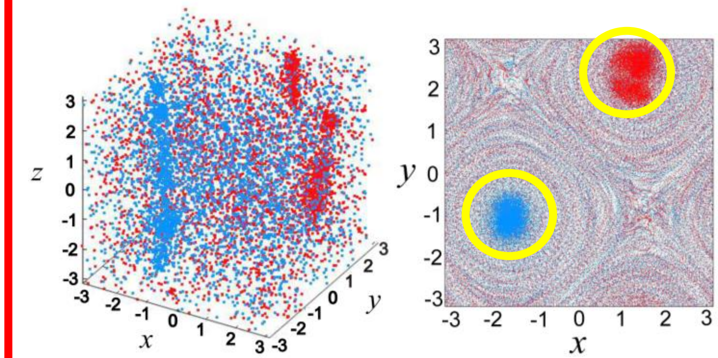

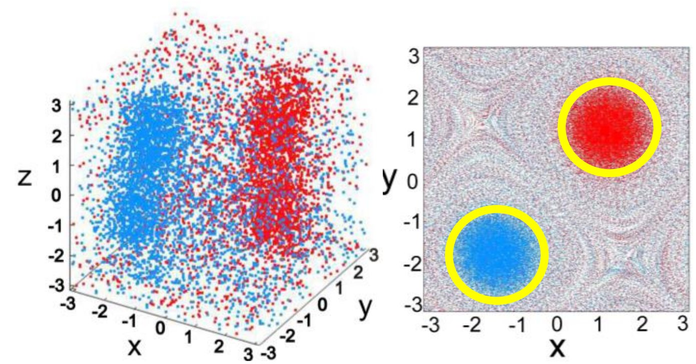

Density based Clustering Analysis

Quantitative analysis of transient process:

DBSCAN method

(Ester *et al. 1996*)

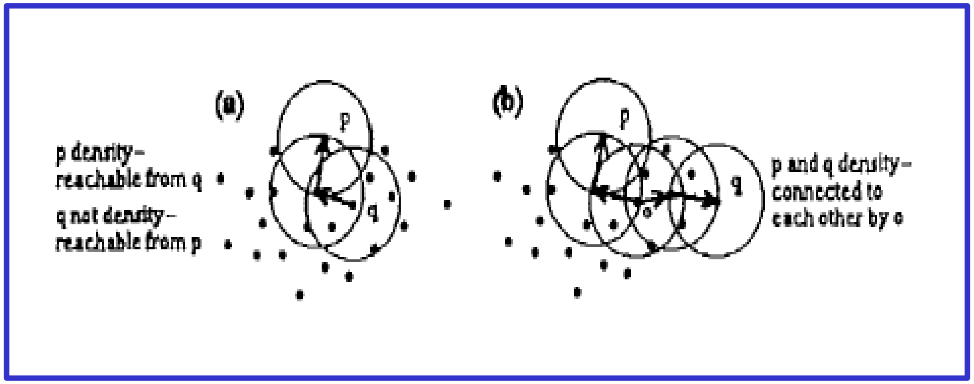

↑ Density based algorithm (Ester *et al*.)

A group of vortices is identified as a cluster, if its size is greater than the minimum radius: r and the number of vortices inside exceeds the minimum number: N_c

Case	r	N_c
A	0.4	25
B	0.4	25
C	0.4	25
D	0.3	22

↑ Used parameters

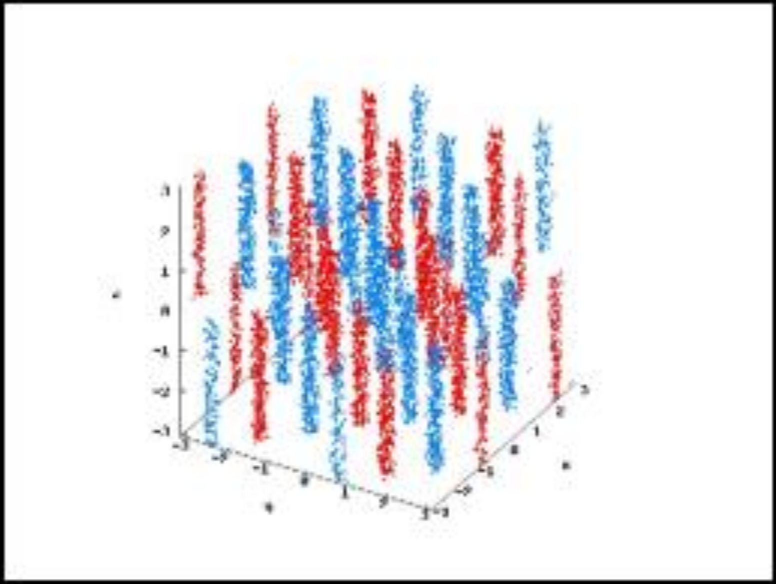
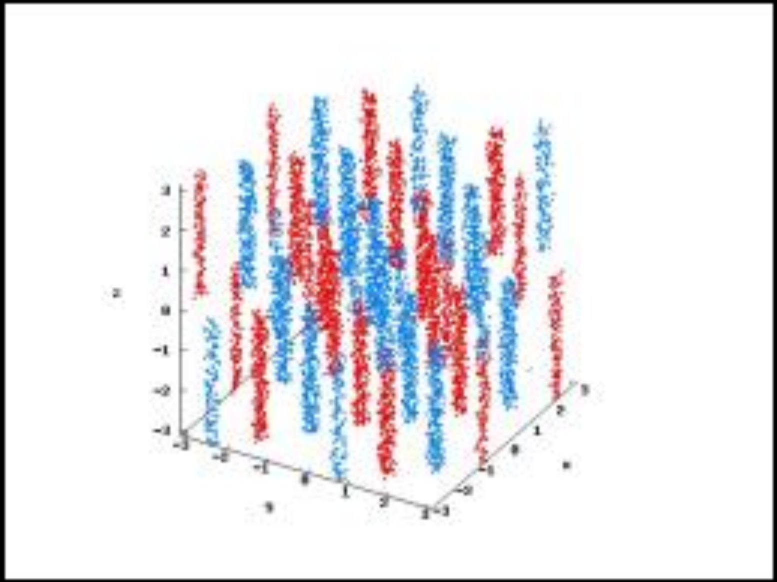
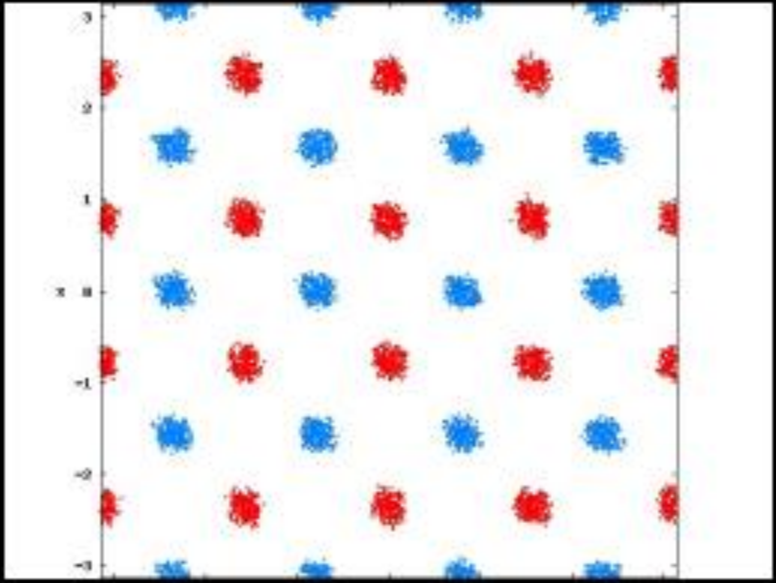
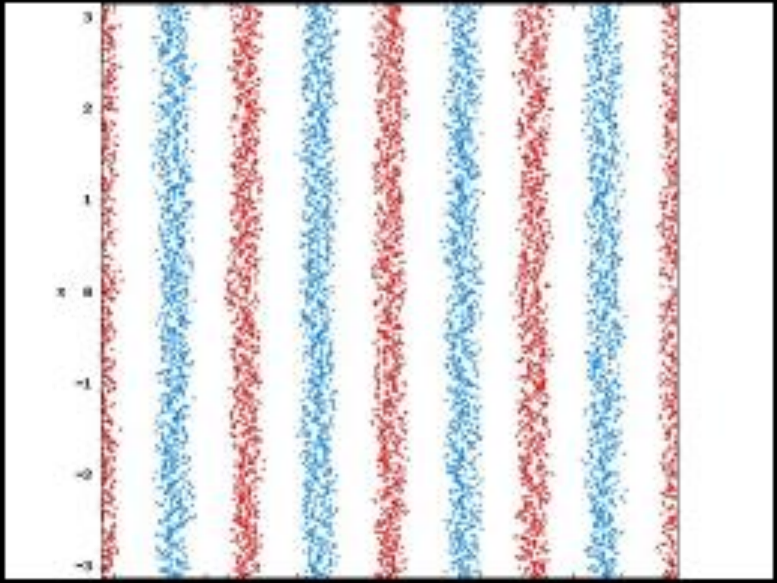

Number of Clusters

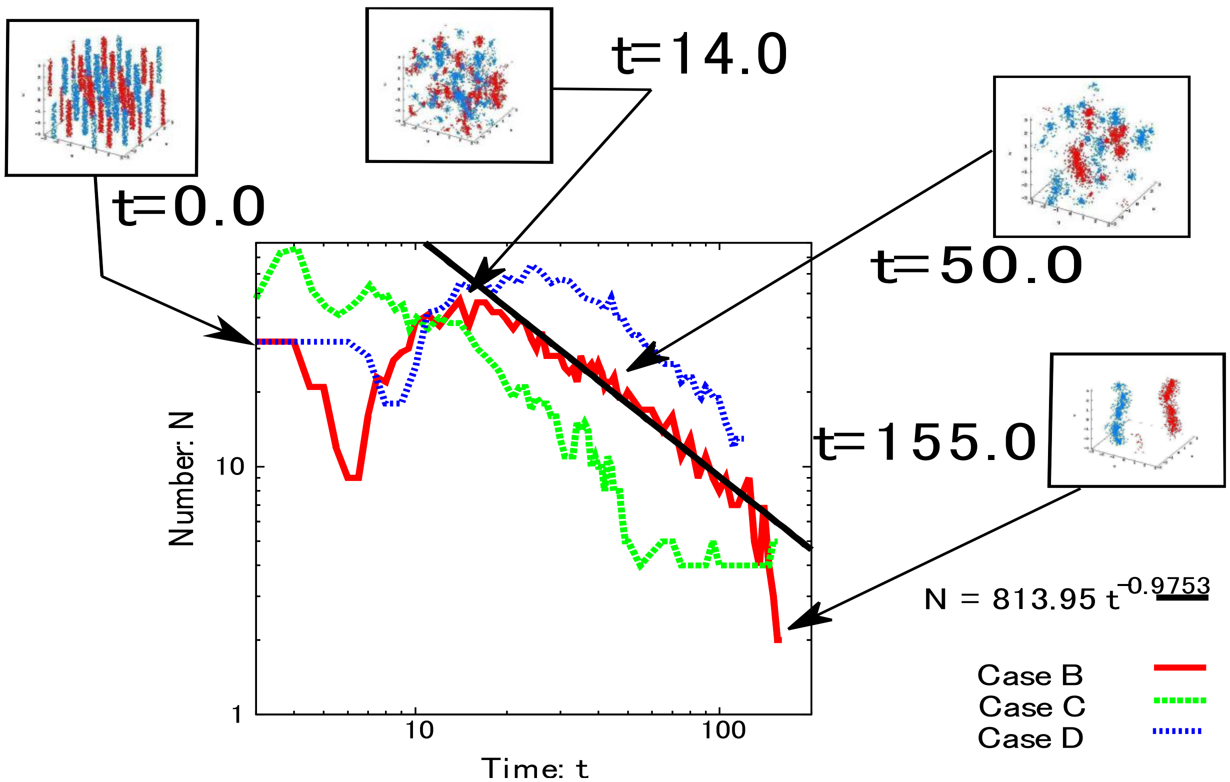

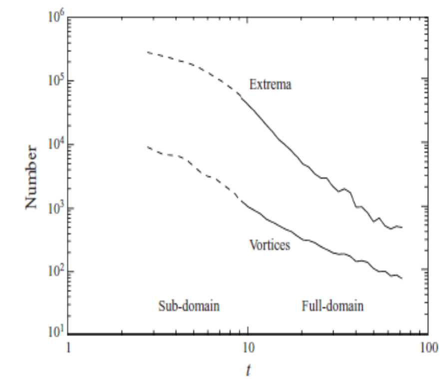

FIGURE 4. The number of extrema and compound vortices, $n_e(t)$ and $n_{cv}(t)$, from the vortex census.

McWilliams *et al.*1999
Spectral Computation

Cluster number decays like t^{-1}, which is slower than in McWilliams' numerical simulations ($t^{-1.25}$).

McWilliams J C, Weiss J B and Yavneh I: *J.Fluid Mech.* **401** 1-16, 1999

Cluster Shape

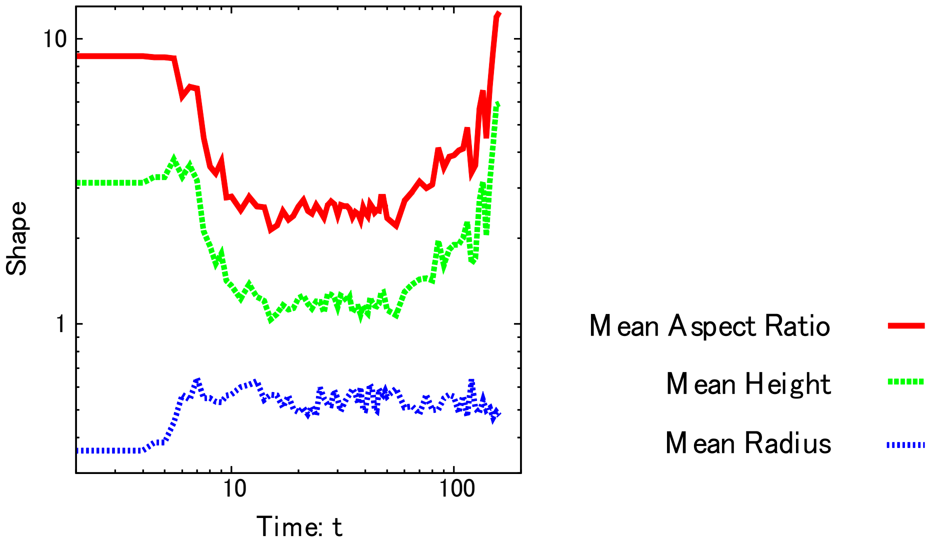

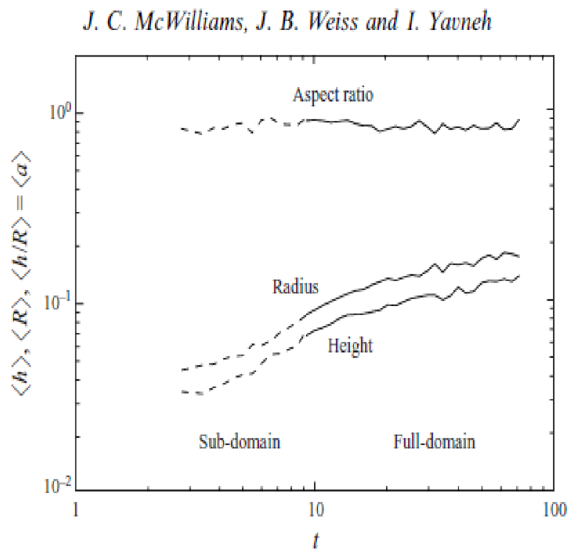

FIGURE 8. The population-mean vortex-element radius, $\langle R \rangle(t)$, half-height, $\langle h \rangle(t)$, and aspect ratio, $\langle a \rangle(t)$, from the vortex census.

- Mean aspect ratio $a = \frac{h}{r}$ of clusters increases with time ($2 \rightarrow 10$).
- Mean radius r remains constant.
- Mean height h increases.

- Mean aspect ratio $a = \frac{h}{r}$ of clusters remains constant (about 1.6).
- Mean radius r increases.
- Mean height h increases.

Clusters align vertically but never merge.

Clusters merge and align.

Maximum Entropy Theory for QG Vortices of Mixed Sign

Conserved quantities

Probability density function: PDF

Vertical vortex distributions

$$P_+(z) = \iint F_+(x,y,z)dxdy \quad , \quad P_-(z) = \iint F_-(x,y,z)dxdy$$

Energy

$$E = \frac{1}{2}\iiiiiint G(\boldsymbol{r},\boldsymbol{r}')[F_+(\boldsymbol{r})F_+(\boldsymbol{r}') + F_-(\boldsymbol{r})F_-(\boldsymbol{r}') - 2F_+(\boldsymbol{r})F_-(\boldsymbol{r}')]d^3\boldsymbol{r}d^3\boldsymbol{r}'$$

Shannon entropy

$$\log \hat{Z} = \frac{1}{N}\log Z = -\iiint [F_+(\boldsymbol{r})\log F_+(\boldsymbol{r}) + F_-(\boldsymbol{r})\log F_-(\boldsymbol{r})]d^3\boldsymbol{r}$$

Lagrange's method of undetermined multipliers

Variational equations

$$\delta F_+ \ : \quad -1 - \log F_+ - \alpha_+(z) - \beta\iiint G(\boldsymbol{r},\boldsymbol{r}')[F_+(\boldsymbol{r}') - F_-(\boldsymbol{r}')]d^3\boldsymbol{r}' = 0$$

$$\delta F_- \ : \quad -1 - \log F_- - \alpha_-(z) - \beta\iiint G(\boldsymbol{r},\boldsymbol{r}')[F_-(\boldsymbol{r}') - F_+(\boldsymbol{r}')]d^3\boldsymbol{r}' = 0$$

$\alpha_\pm(z) \Rightarrow P_\pm(z)$

$\beta \Rightarrow E$

Turkington .B & Whitaker .N : SIAMJ. Sci. Comput. (1996)

Funakoshi, S. & Miyazaki, T.,: Fluid Dyn. Res. 44 (2012)

Mean Field Equation for QG Point Vortices

- For Quasi-geostrophic point vortices

Potential vorticity : $q(\boldsymbol{r}) \equiv F_+(\boldsymbol{r}) - F_-(\boldsymbol{r})$

Stream function : $\psi(\boldsymbol{r}) \equiv \iiint G(\boldsymbol{r},\boldsymbol{r}')[F_+(\boldsymbol{r}') - F_-(\boldsymbol{r}')]d^3\boldsymbol{r}'$

- **Symmetric case:** $\alpha_+(z) = \alpha_-(z) = \alpha(z)$
- **The maximum entropy state satisfies the following equation:**

$$q(\boldsymbol{r}) = -2e^{-\alpha(z)-1}\sinh\beta\psi(\boldsymbol{r})$$

Potential vorticity: $q(\boldsymbol{r}) = -\Delta\psi(\boldsymbol{r})$

Mean field equation

$$\Delta\bar{\psi}(\boldsymbol{r}) + \lambda^2(z)\sinh\bar{\psi}(\boldsymbol{r}) = 0$$

$*\ \bar{\psi}(\boldsymbol{r}) = \beta\psi(\boldsymbol{r})$, $\lambda^2(z) = -2\beta e^{-\alpha(z)-1}$

- It reduces to the Sinh-Poisson equation for 2D point vortices

$$\Delta\psi(\boldsymbol{r}) + \lambda^2\sinh\psi(\boldsymbol{r}) = 0$$

Joyce & Montgomery : J. Plasma Phys. (1973)

Dual Problem of the Maximum Entropy Theory

Dual problem

$$\alpha_+^{k+1}(z)P_+(z) + \alpha_-^{k+1}(z)P_-(z) + \beta^{k+1}(E^k + E_0)$$
$$+ \iiint \exp\left[-1 - \alpha_+^{k+1}(z) - \beta^{k+1}\psi^k(\boldsymbol{r})\right] d^3\boldsymbol{r} + \iiint \exp\left[-1 - \alpha_-^{k+1}(z) + \beta^{k+1}\psi^k(\boldsymbol{r})\right] d^3\boldsymbol{r}$$

⇒ **Minimum**

Conserved quantities

$$\begin{cases} P_+(z) = \iint \exp\left[-1 - \alpha_+^{k+1}(z) - \beta^{k+1}\psi^k(\boldsymbol{r})\right] dxdy = \iint F_+^{k+1}(\boldsymbol{r})dxdy \\ P_-(z) = \iint \exp\left[-1 - \alpha_-^{k+1}(z) + \beta^{k+1}\psi^k(\boldsymbol{r})\right] dxdy = \iint F_-^{k+1}(\boldsymbol{r})dxdy \\ E^k + E_0 = \iiint \psi^k\{F_+^{k+1}(\boldsymbol{r}) - F_-^{k+1}(\boldsymbol{r})\} d^3\boldsymbol{r} \end{cases}$$

Where, $\Delta\psi^k(\boldsymbol{r}) = -F_+^k(\boldsymbol{r}) + F_-^k(\boldsymbol{r})$

- Assuming $F_+^k, F_-^k, \alpha_+^k(z), \alpha_-^k(z), \beta^k$ are given,
- determine $\alpha_+^{k+1}(z), \alpha_-^{k+1}(z), \beta^{k+1}$ by an iteration method.

Accuracy: $EPS = \sum_{i=1}^{n}[|\alpha_+^{k+1}(z(i)) - \alpha_+^k(z(i))|^2 + |\alpha_-^{k+1}(z(i)) - \alpha_-^k(z(i))|^2 + |\beta^{k+1} - \beta^k|^2] \leq 10^{-8}$

Turkington .B & Whitaker .N : SIAMJ. Sci. Comput. (1996)

Comparison between Numerical and Theoretical Results

◆Numerical results by point vortex simulation

caseA E=6.413×10^{-3} **caseB E=2.424×10^{-3}** **caseC E=2.714×10^{-3}**

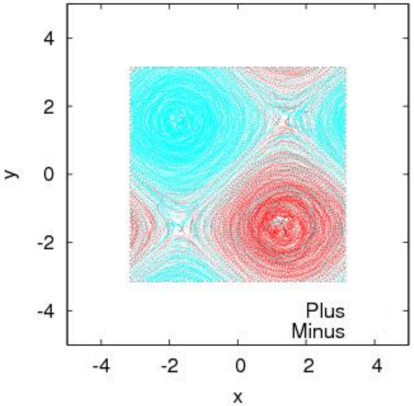

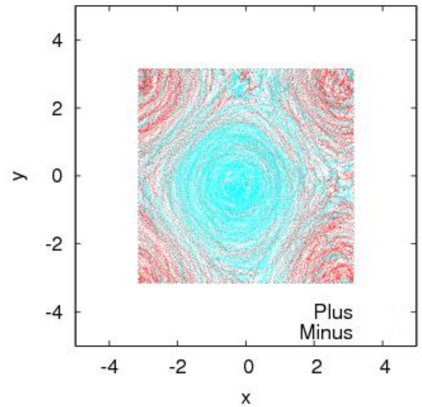

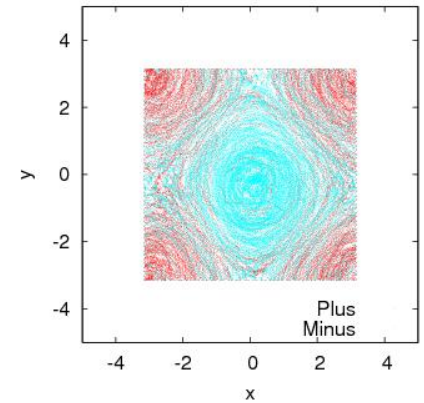

◆Theoretical results : initial potential vorticity ➡ numerical results

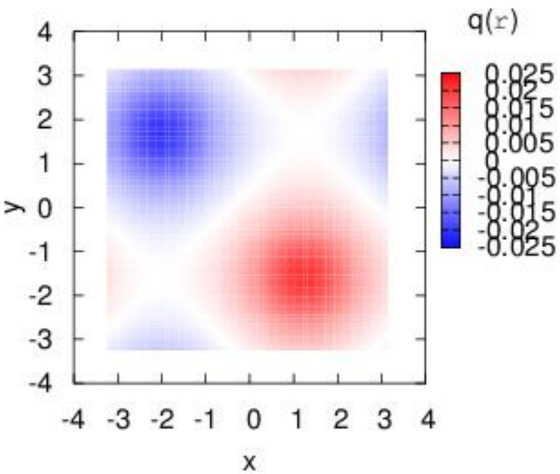

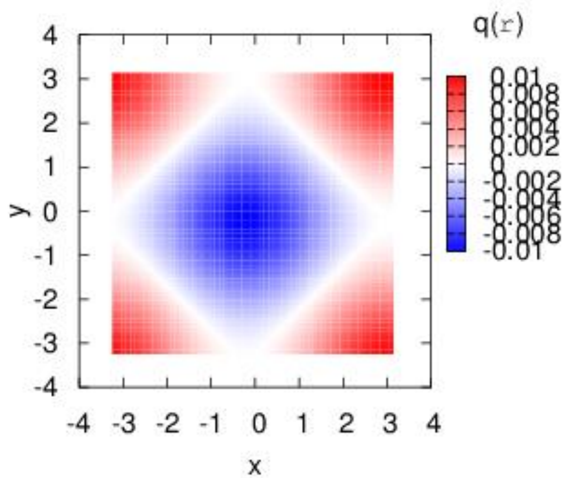

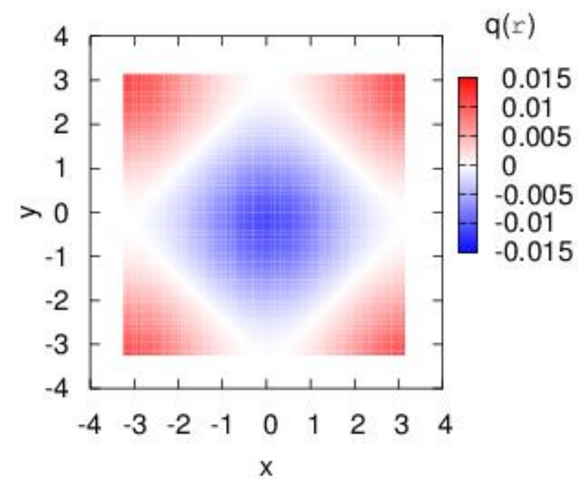

E=6.413×10^{-3} **E=2.424×10^{-3}** **E=2.714×10^{-3}**

✓ **Numerical equilibriums are Maximum entropy states !**

2D Exact Solutions

- Diagram in *E*-*S* plane: Cases A∼C

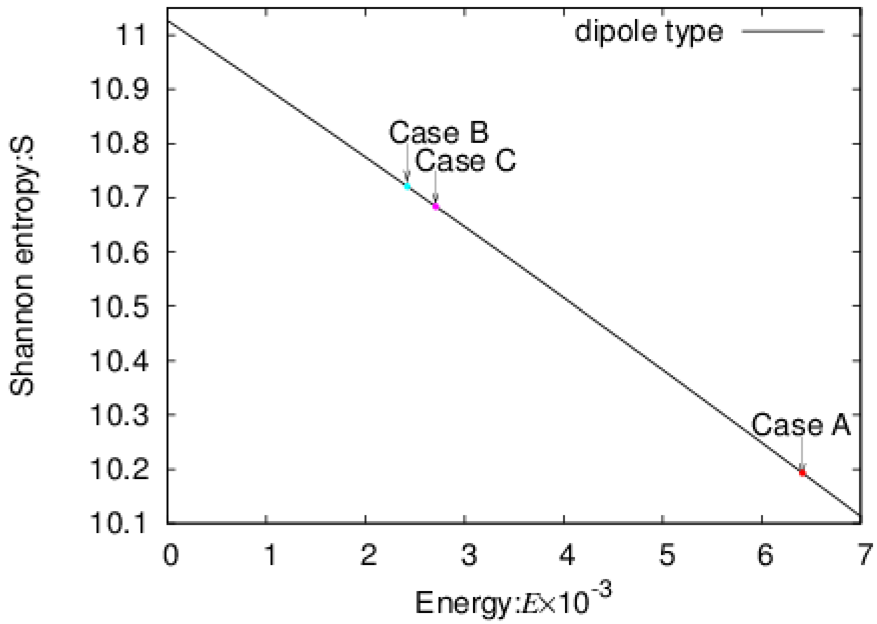

Cases A∼C are on the same branch.

"Sinh-Poisson Eq." has Soliton solutions.

- Stream function

Case B : $\lambda^2(z) = 0.8852, \quad k = 0.02074$

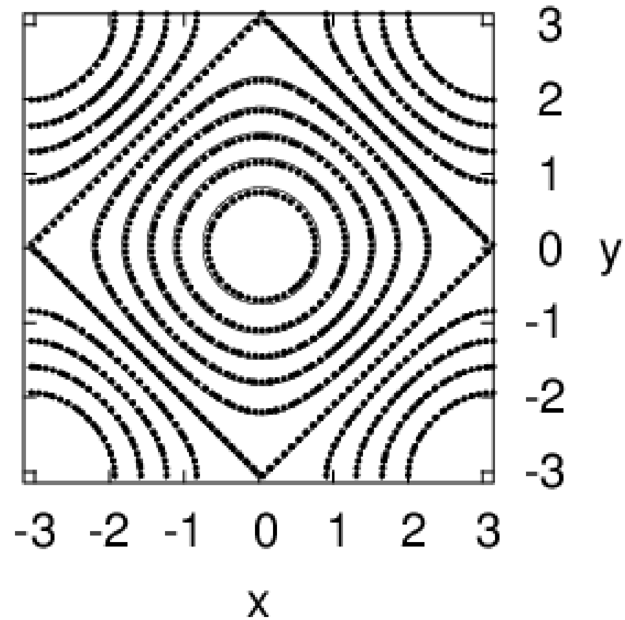

Cases A∼C are two-dimensional "sn-sn dipole"-type solutions.

$$\Psi = 4\tanh^{-1}\left[\frac{\sqrt{k}sn(rx,k) - \sqrt{k_1}sn(sy,k_1)}{1+\sqrt{kk_1}sn(rx,k)sn(sy,k_1)}\right]$$

$$s^2(1-k_1)^2 = \lambda^2 + 4r^2k, \quad s(1+k_1) = r(1+k)$$

Gurarie & Chow : Phys. Fluids. (2004)

2π-Cubic box

$$s = r = 2K(k)/\pi$$

$$k = k_1$$

Elliptic integral : $K(k)$

Elliptic function : $sn(u,k)$

Other Maximum Entropy States ?

Initial vorticity guess	Vortex type	Vertical distribution: P(z)
$A\ sinx$	zonal flow (2D)	$1/(2\pi)$
$A\ (cosx + cosy)$	dipole (2D)	$1/(2\pi)$
$A\ sinxsiny$	quadrupole (2D)	$1/(2\pi)$
$A\ sinx\ sinz$	zonal flow (3D)	$1/(2\pi)$
$A\ (cosx + cosy)sinz$	dipole (3D)	$1/(2\pi)$
$A\ sinxsinysinz$	quadrupole (3D)	$1/(2\pi)$

Numerical Results

Bifurcation Diagram in the *E-S* plane: 2D and 3D Maximum Entropy States

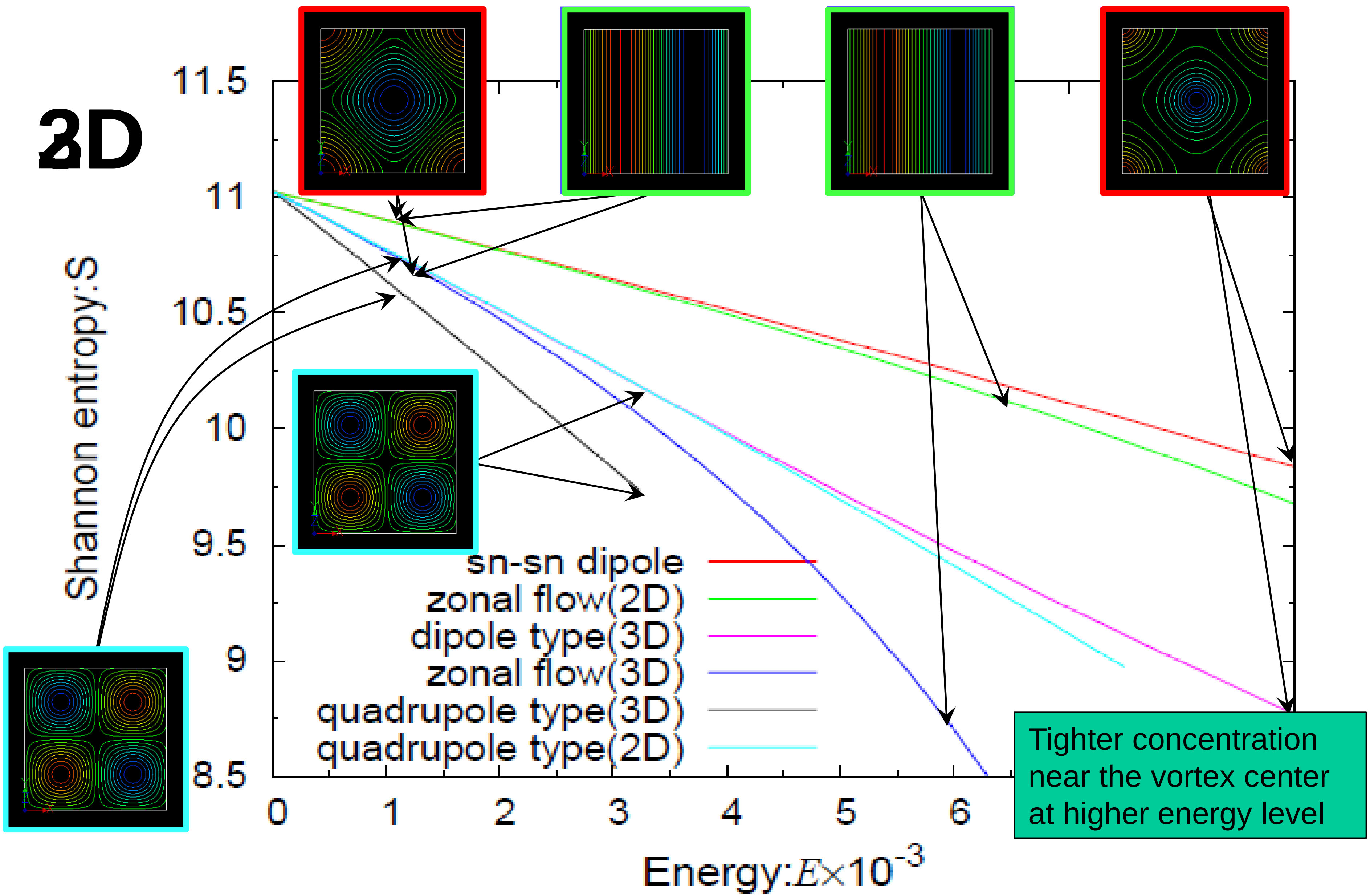

Transition to Maximum Entropy State

Box size: $L_x : L_y : L_z = 2\pi : 2\pi : 2\pi$

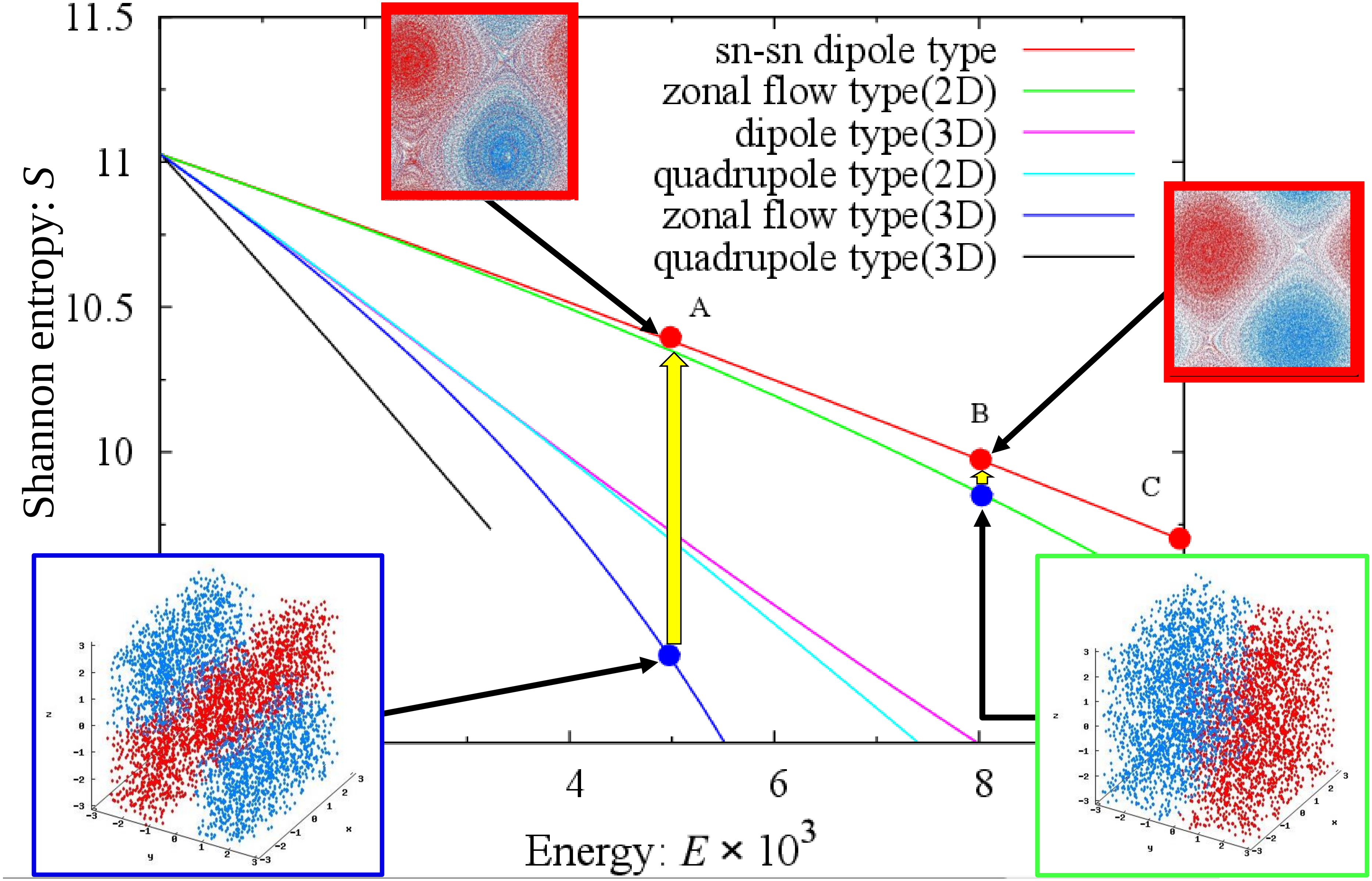

Entropy Growth

∗ Entropy Evaluation

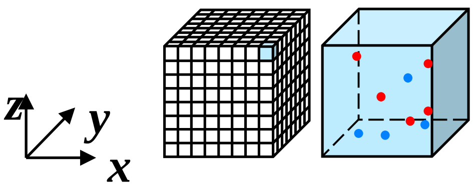

$$\nabla V = \frac{(2\pi)^3}{N} \qquad F_{\pm}(\boldsymbol{r}) = \frac{n_{\pm}}{N\Delta V} = \frac{n_{\pm}}{(2\pi)^3}$$

$$S = -\iiint [F_+(\boldsymbol{r}) \log F_+(\boldsymbol{r}) + F_-(\boldsymbol{r}) \log F_-(\boldsymbol{r})] d^3\boldsymbol{r}$$

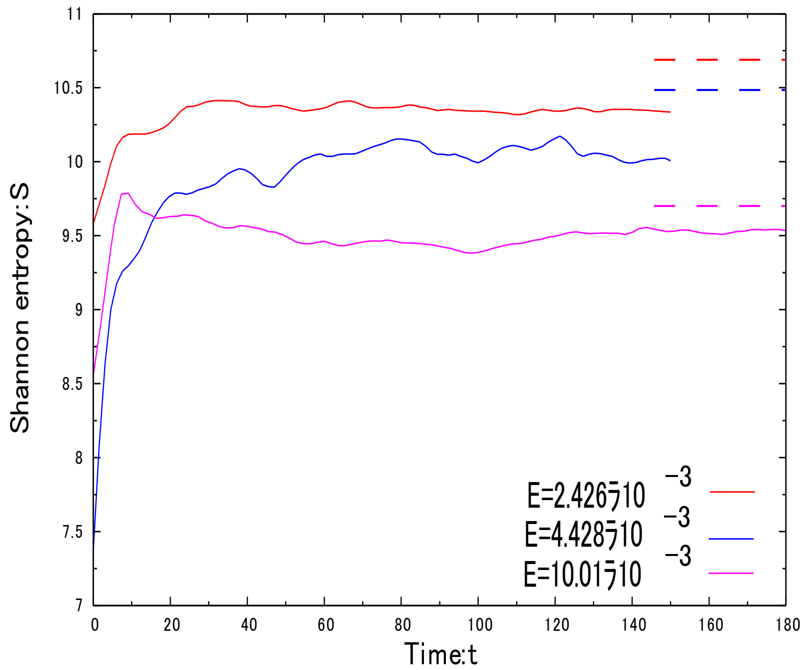

Shannon entropy grows with time and seems to approach the equilibrium value from below.

Stability Analysis by Arnold's Method

Conserved Quantities

$$H = \frac{1}{2}\iiint q\psi\, dx\,dy\,dz\,, \quad C = \iiint F(q,z)\, dx\,dy\,dz$$

$$\psi \leftarrow \psi_0 + \delta\psi$$

Equilibrium — Disturbance

variations of $H_C = H + C$

$$-F(q_0, z) = q_0 \sinh^{-1}\left(\frac{q_0}{\lambda^2(z)}\right) - \sqrt{\lambda^4(z) + q_0^2}$$ **to have the Mean Field Equation**

First variation: $$\delta H_C = \iiint \left[q_0 - \Delta\left(\frac{\partial F}{\partial q_0}\right)\right]\delta\psi\, dx\,dy\,dz = 0$$

Second variation: $$\delta^2 H_C = \frac{1}{2}\iiint \left[|\mathrm{grad}\,\delta\psi|^2 - \frac{(\Delta(\delta\psi))^2}{\sqrt{\lambda^4(z) + q_0^2}}\right] dx\,dy\,dz \;\;?\;\; 0$$

Stability cannot be proved in general

Results of Stability Analysis

2D

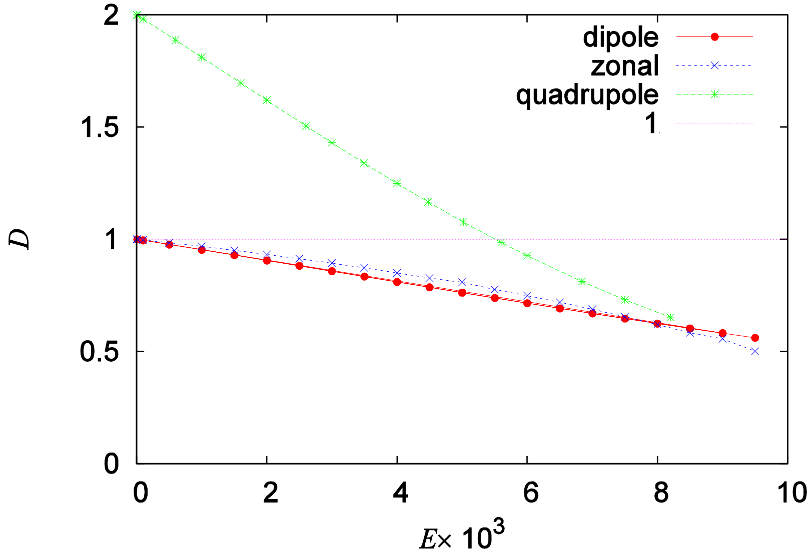

Less than 1 for 2D-dipole and 2D-zonal: “Stable”
More than 1 for 2D-quadrupole: “Possibly Unstable”

3D

3D-dipole

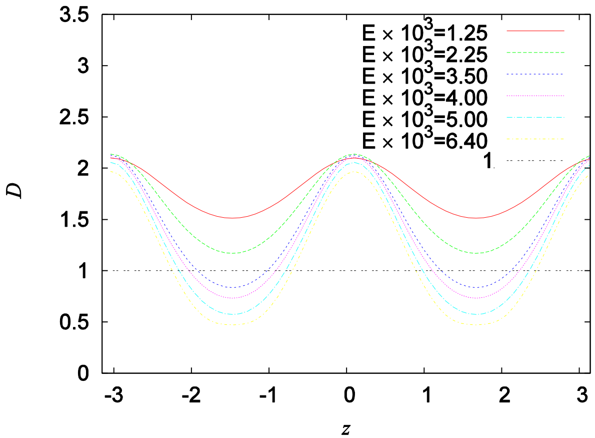

3D-zonal

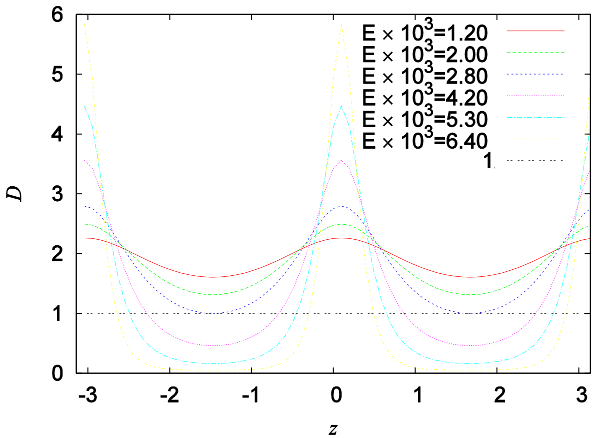

3D-quadrupole

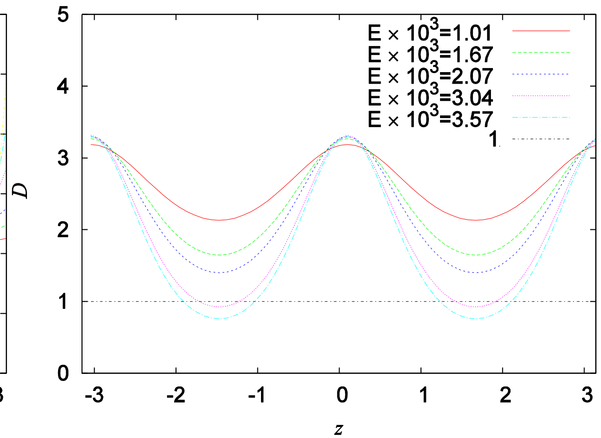

More than 1 for any case : “Possibly Unstable”

Direct Numerical Simulations of QG equation

Continuous QG equation

ν : Viscosity

p : Order of dissipation

$$\left(\frac{\partial}{\partial t} + \frac{\partial \psi(\boldsymbol{r},t)}{\partial y}\frac{\partial}{\partial x} - \frac{\partial \psi(\boldsymbol{r},t)}{\partial x}\frac{\partial}{\partial y}\right) q(\boldsymbol{r},t) = \underline{(-1)^{p+1}\nu\Delta^p q(\boldsymbol{r},t)}$$

Dissipation term

Fourier Modes (Quasi-Spectral Method)

$$\hat{q}(k_x, k_y, k_z, t) = (k_x^2 + k_y^2 + k_z^2)\hat{\psi}(k_x, k_y, k_z, t)$$

Wave number vector: $\boldsymbol{k} = (k_x, k_y, k_z)$

Initial Equilibrium States

①

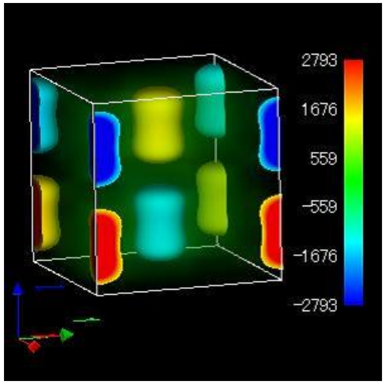

3D-dipole

E＝6.40×10^{-3}

②

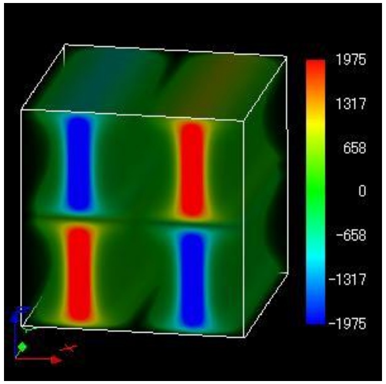

3D-zonal

E＝6.40×10^{-3}

Adding small disturbances
4th order RK time marching
De-aliasing by 2/3 rule

Results of Direct Numerical Simulations of QG equation

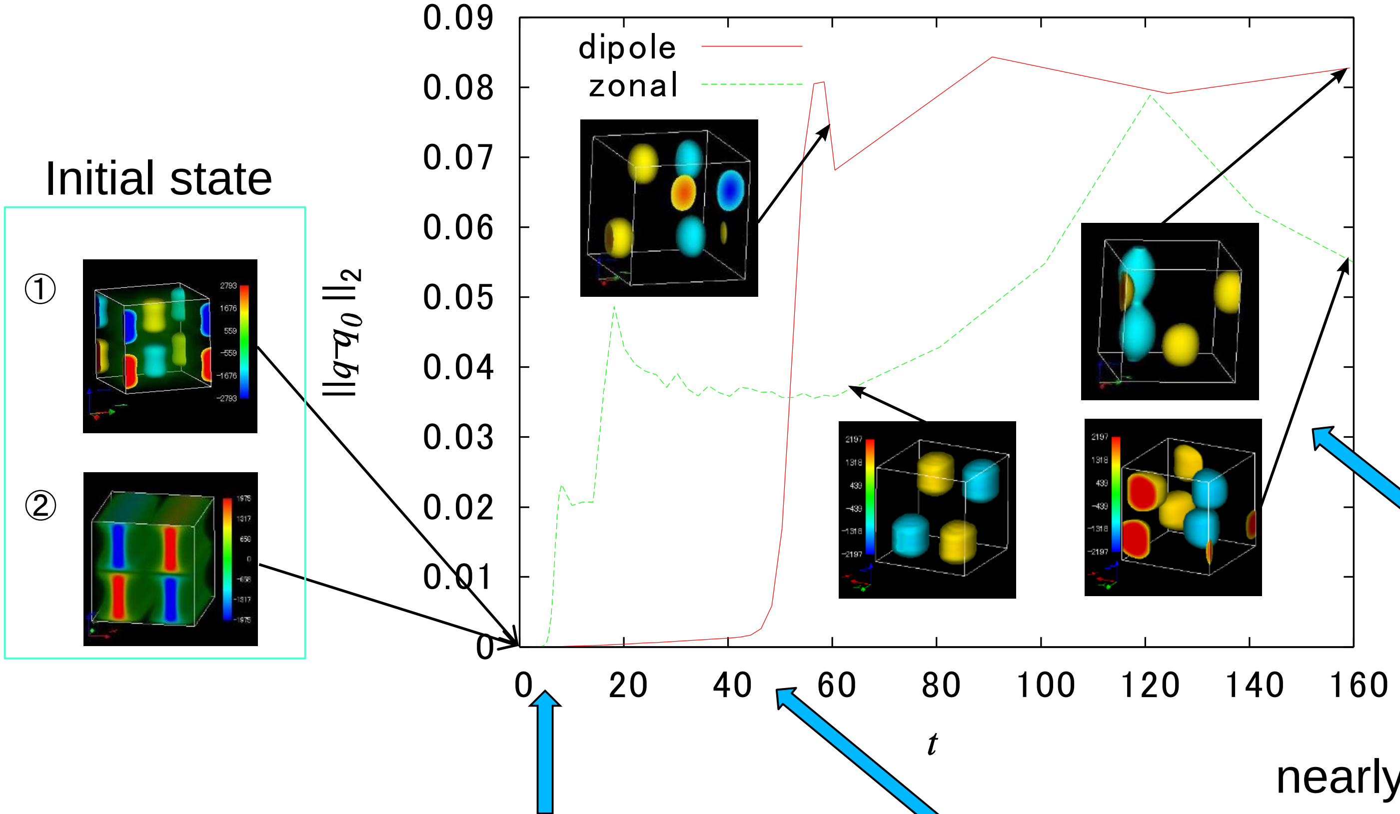

nearly 2D pattern appears

After t= 10, the zonal structure becomes wavy and a quadrupole-like structure develops by t=60

A drastic deviation is observed after t= 40

Summary

- We investigate the statistical mechanics of bi-disperse quasi-geostrophic point vortices numerically and theoretically.

1. Clustering of vortices of like sign occurs (negative temperature state), and the equilibrium has two-dimensional dipole structure.
2. Shannon entropy increases and the number of cluster decreases like t^{-1}.
3. The maximum entropy states are determined theoretically by solving the mean field equation. They coincide with the numerical end states.
4. Two- and three-dimensional maximum entropy states are found.
5. The two-dimensional *sn*-*sn* dipole solution has the largest entropy, which is the reason only this branch is found numerically.
6. The two-dimensional *sn*-*sn* dipole and zonal flow solutions are found to be stable.

Thank you for your attention

Entropy Growth in Numerical Simulations

Shannon Entropy

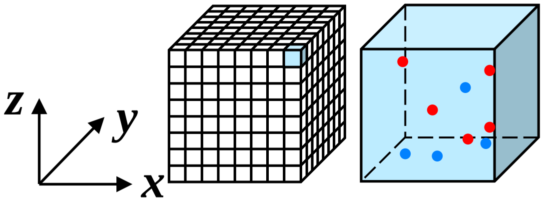

$$\nabla V = \frac{(2\pi)^3}{N} \qquad F_{\pm}(\boldsymbol{r}) = \frac{N_{\pm}}{N\nabla V} = \frac{N_{\pm}}{(2\pi)^3}$$

$$S = -\iiint [F_{+}(\boldsymbol{r}) \log F_{+}(\boldsymbol{r}) + F_{-}(\boldsymbol{r}) \log F_{-}(\boldsymbol{r})] d^3\boldsymbol{r}$$

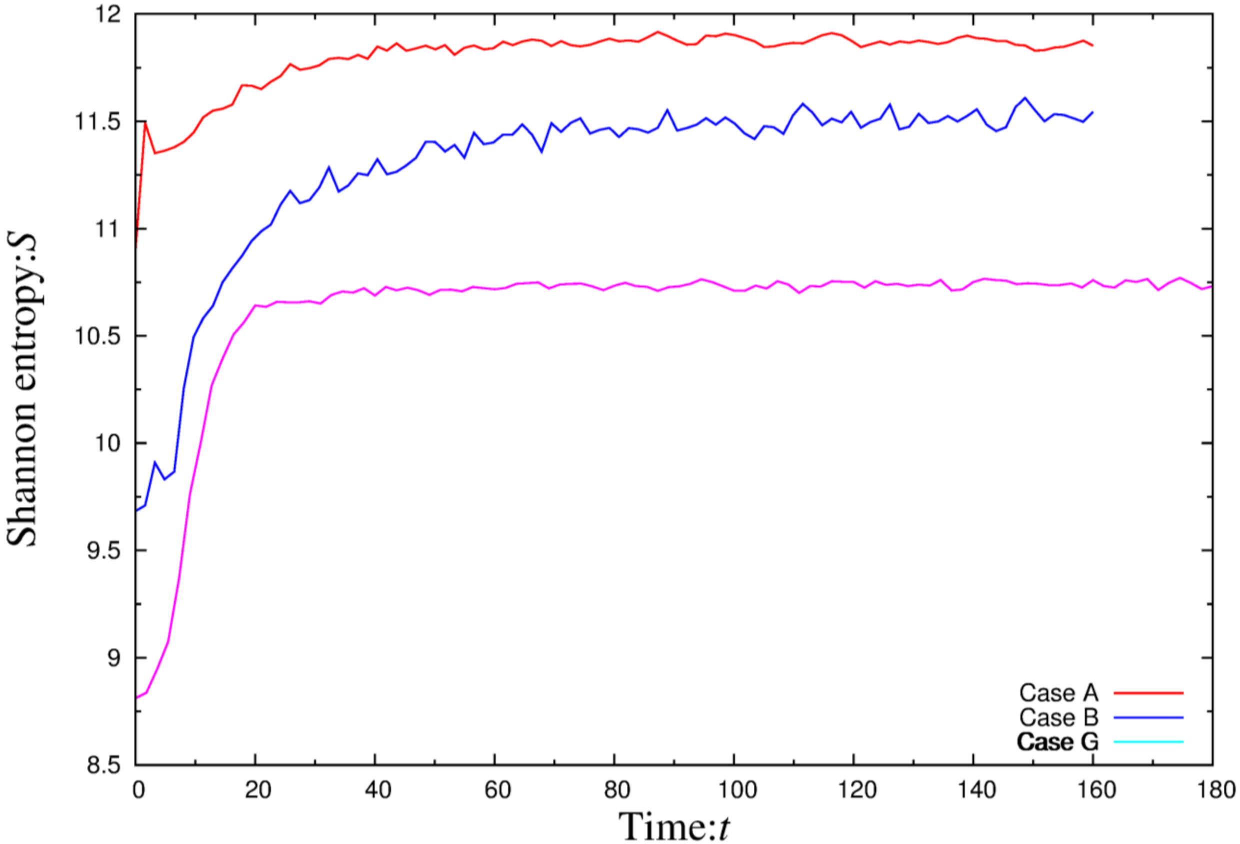

Ewald Sum : Energy under periodic boundary conditions

- **Energy (Hamiltonian)**

$$H = H^{(1)} + H^{(2)} + H^{(3)}$$

Real space — Wavenumber space — Constant term

Assume: $F(r) = \Gamma' \left(\frac{\alpha}{\pi}\right)^{\frac{3}{2}} \exp(-\alpha^2 r^2)$: **Gaussian**

($\alpha[\mathrm{L}^{-1}]$: **scaling parameter)**

[**for cubic cell** L^3] $L = \pi - (-\pi) = 2\pi$

- **Real space**

$$H^{(1)} = \frac{1}{2} \sum_{n} \sum_{i} \sum_{j}{}' \frac{\hat{\Gamma}_i \hat{\Gamma}_j}{4\pi} \frac{\mathrm{erfc}(\alpha |\boldsymbol{R}_i - \boldsymbol{R}_j + L\boldsymbol{n}|)}{|\boldsymbol{R}_i - \boldsymbol{R}_j + L\boldsymbol{n}|}$$

- **Wavenumber space**

$$H^{(2)} = \frac{2\pi}{L^3} \sum_{\boldsymbol{G} \neq 0} \frac{\exp(-|\boldsymbol{G}|^2/4\alpha^2)}{|\boldsymbol{G}|} \sum_{i} \sum_{j} \frac{\hat{\Gamma}_i \hat{\Gamma}_j}{4\pi} \cos\{\boldsymbol{G} \cdot (\boldsymbol{R}_i - \boldsymbol{R}_j)\}$$

- **Self energy (Constant term)**

$$H^{(3)} = -\sum_{i} \frac{\hat{\Gamma}_i^2}{4\pi} \frac{\alpha}{\sqrt{\pi}}$$

Canonical equations of motion for the i−th vortex

$$\frac{\mathrm{d}X_i}{\mathrm{d}t} = \frac{1}{\hat{\Gamma}_i} \frac{\partial H}{\partial Y_i}, \qquad \frac{\mathrm{d}Y_i}{\mathrm{d}t} = -\frac{1}{\hat{\Gamma}_i} \frac{\partial H}{\partial X_i}$$

$$E = H / (\textstyle\sum_{i=1}^{N} |\hat{\Gamma}_i|)^2$$

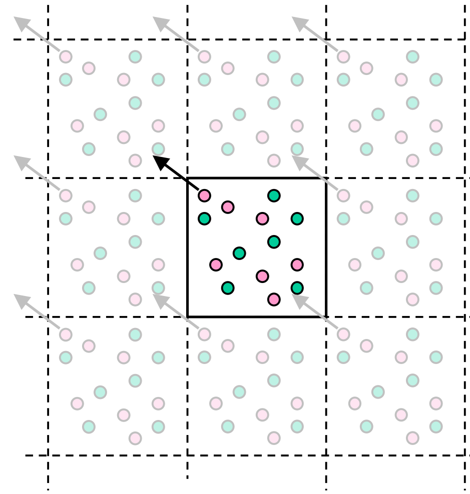

Real space and image cells

$\boldsymbol{G} = \frac{2\pi}{L} \boldsymbol{h}$: **wavenumber vector (** h **: integer vector)**

Influence of Aspect ratio: $L_z / L_x = 0.5$ and 4.0

Box size:

$$L_x : L_y : L_z = 2\pi : 2\pi : \pi$$

Entropy decrease of 3D solutions

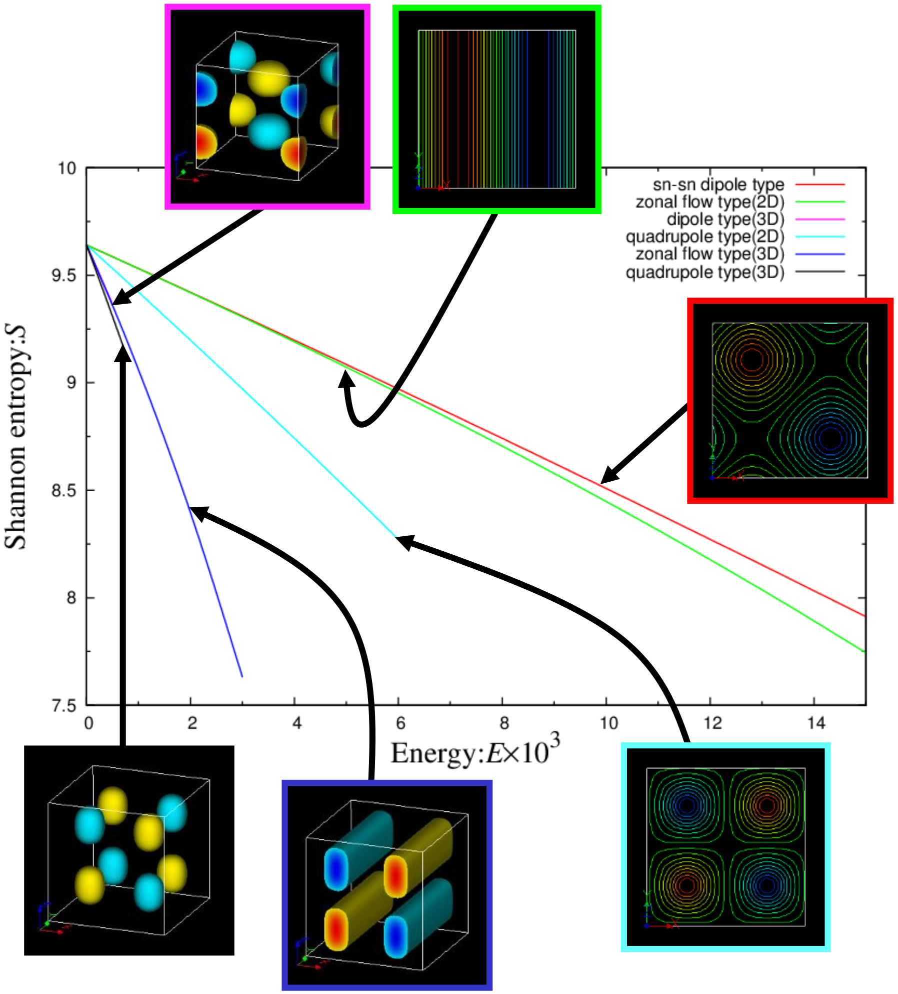

$$L_x : L_y : L_z = 2\pi : 2\pi : 8\pi$$

Entropy increase of 3D solutions

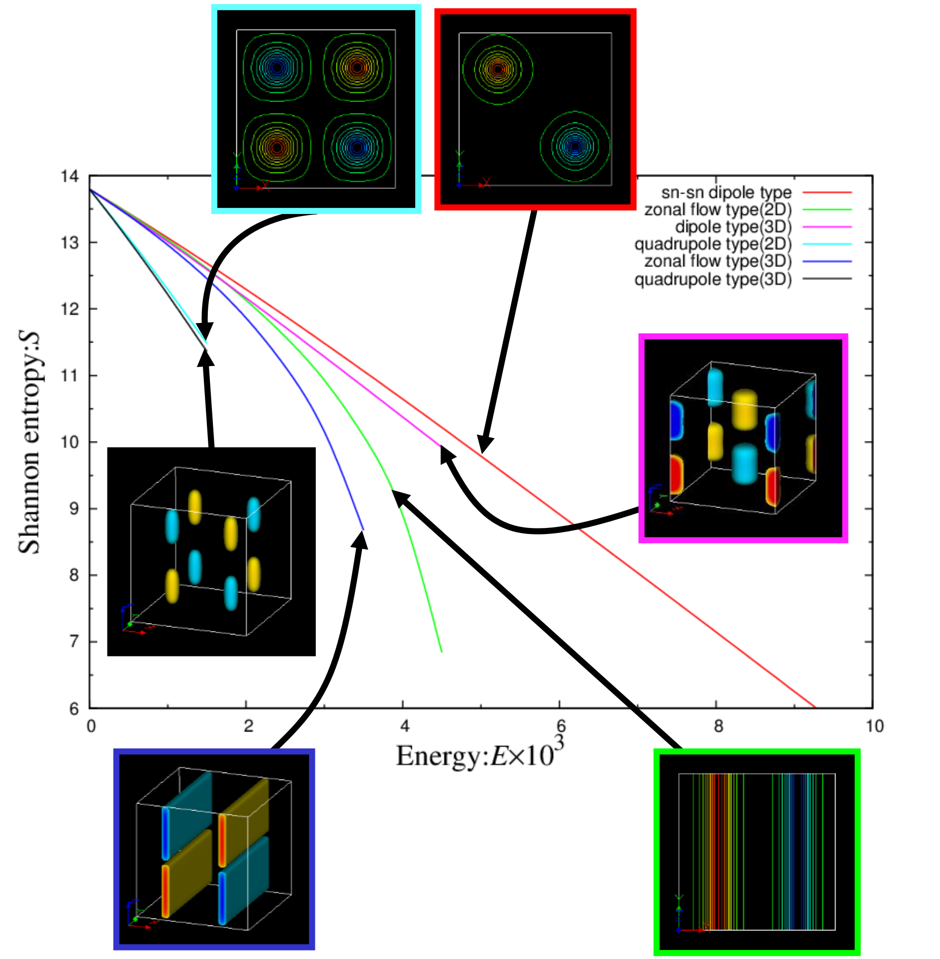

Two types of Zonal Flow for $L_y / L_x = 0.9$

Box size: $L_x : L_y : L_z = 2\pi : 1.8\pi : 2\pi$

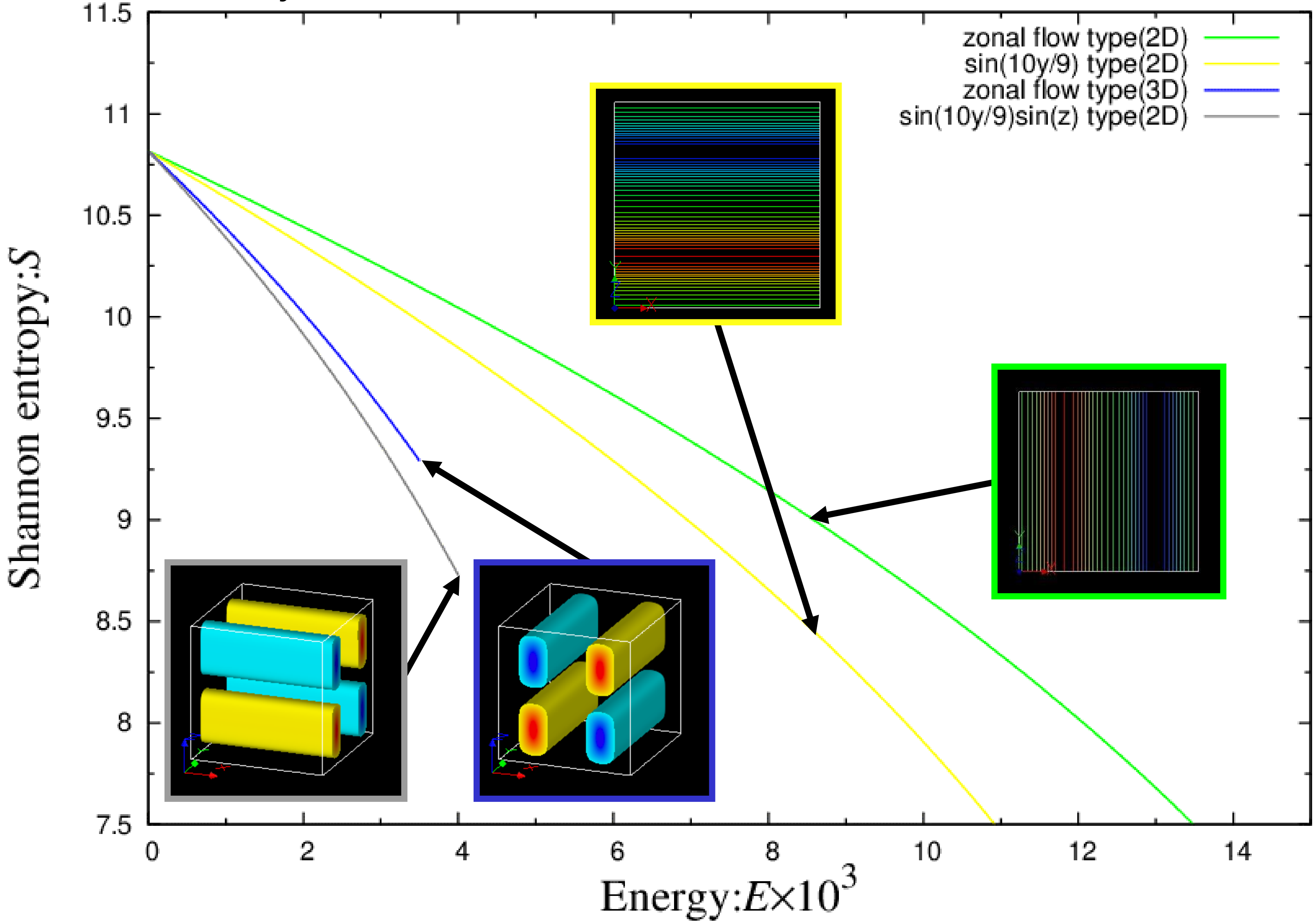

Influence of Aspect ratio: $L_y / L_x = 0.8$

Box size: $L_x : L_y : L_z = 2\pi : 1.6\pi : 2\pi$

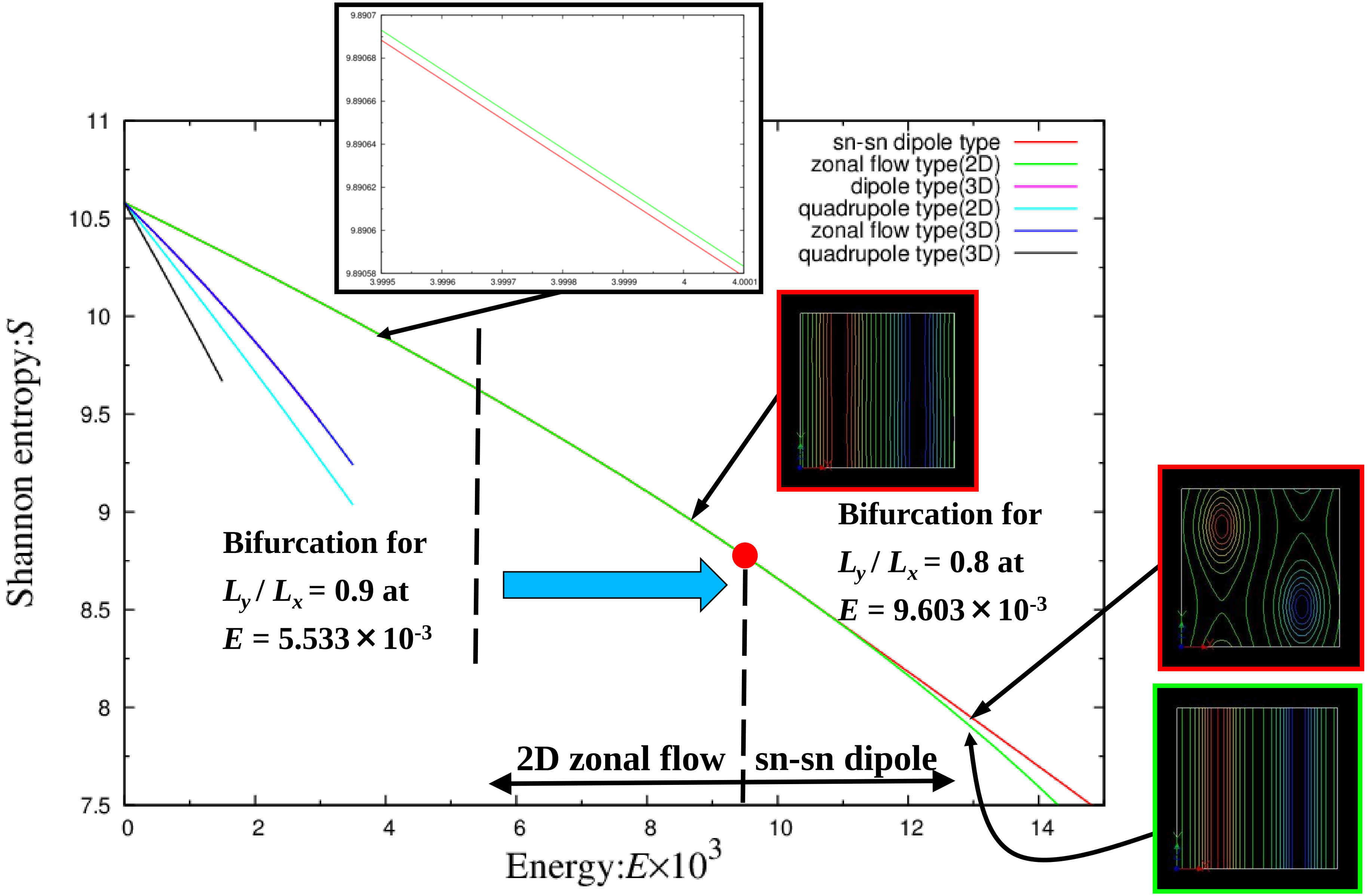

Influence of Aspect ratio: $L_y / L_x = 0.5$

Box size: $L_x : L_y : L_z = 2\pi : \pi : 2\pi$

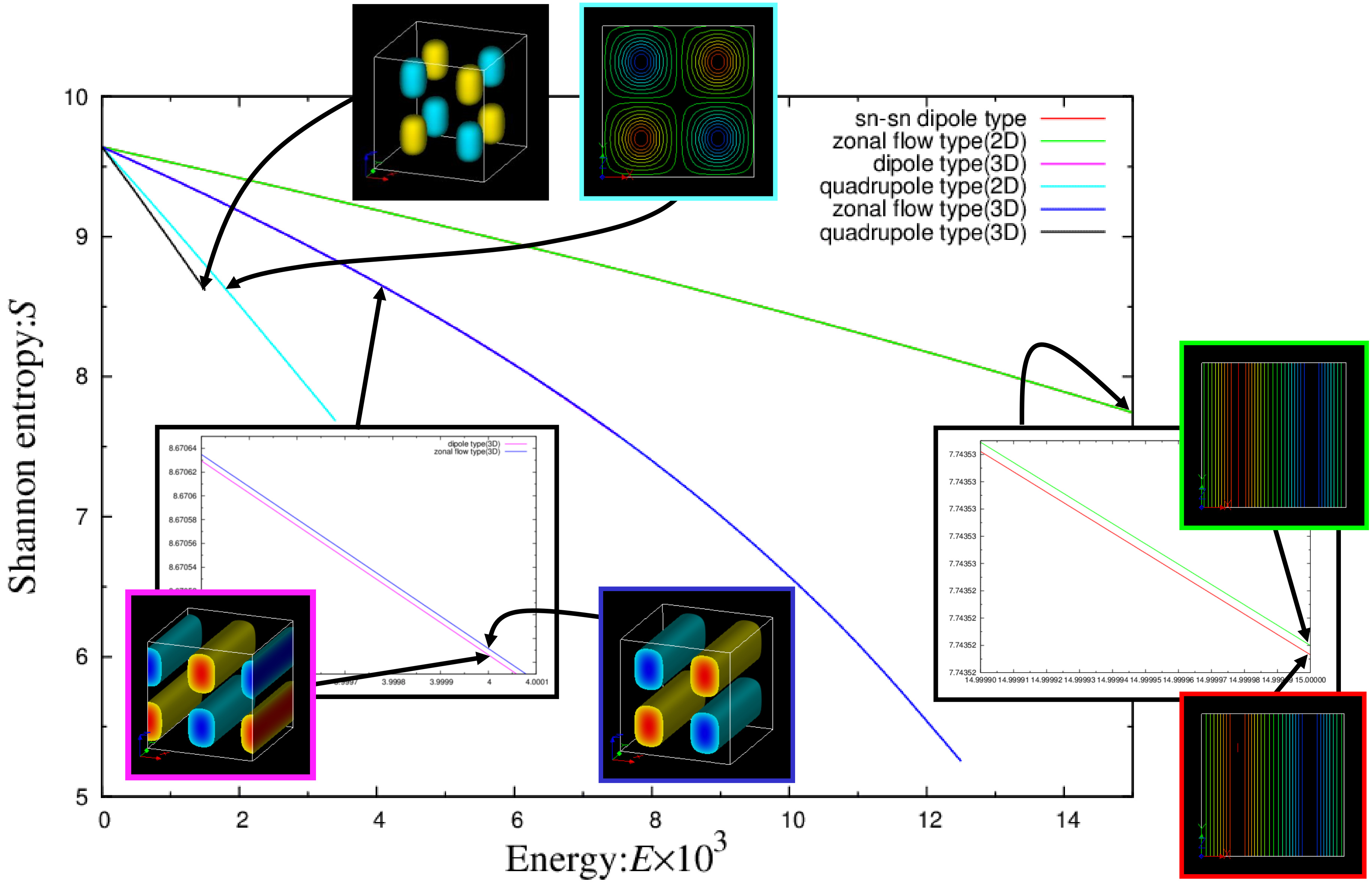

Influence of Aspect ratio: $L_y / L_x = 0.9$

Box size: $L_x : L_y : L_z = 2\pi : 1.8\pi : 2\pi$

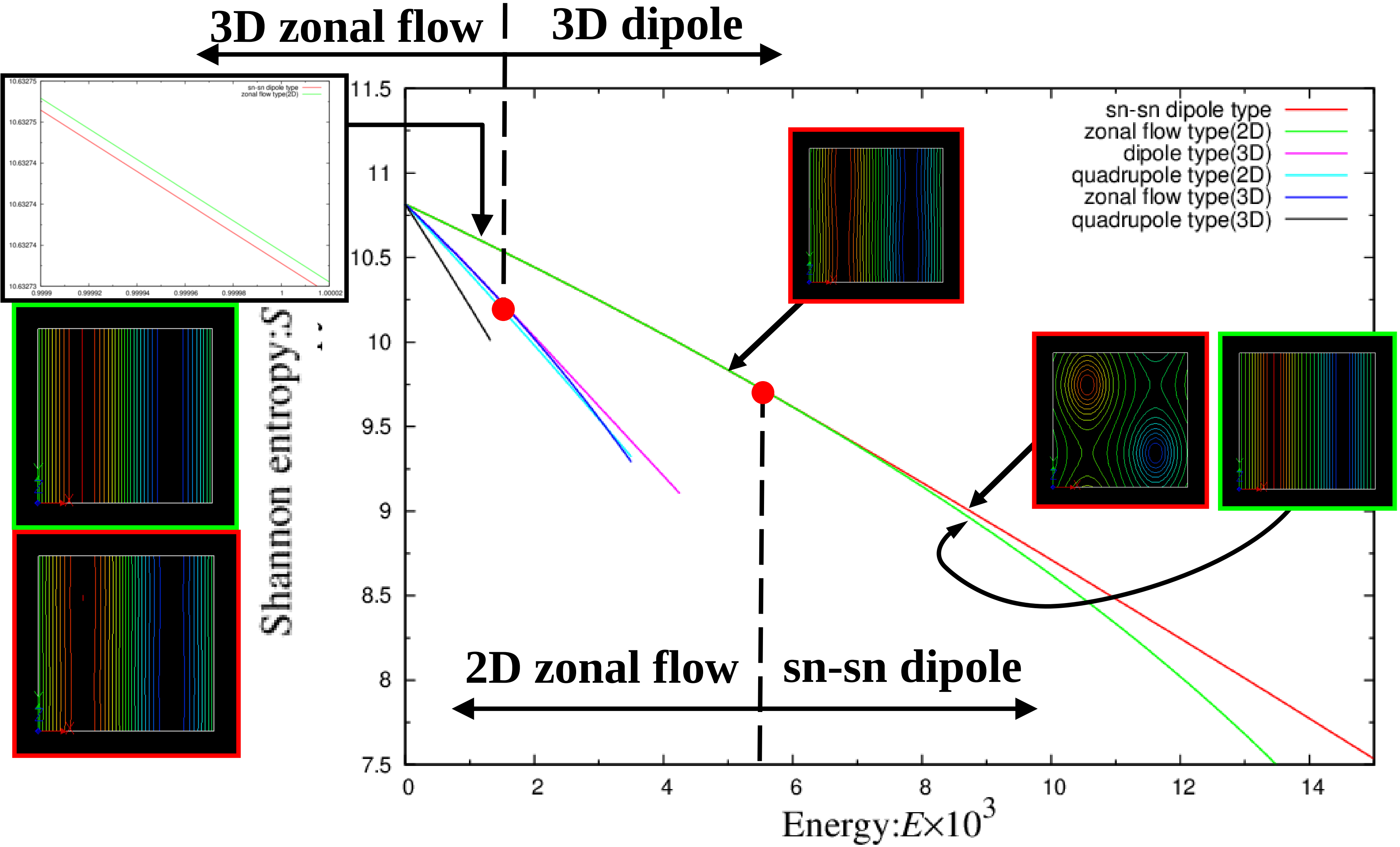

Influence of Aspect ratio: $L_y / L_x = 0.9$, $L_z / L_x = 4.0$

Box size: $L_x : L_y : L_z = 2\pi : 1.8\pi : 8\pi$

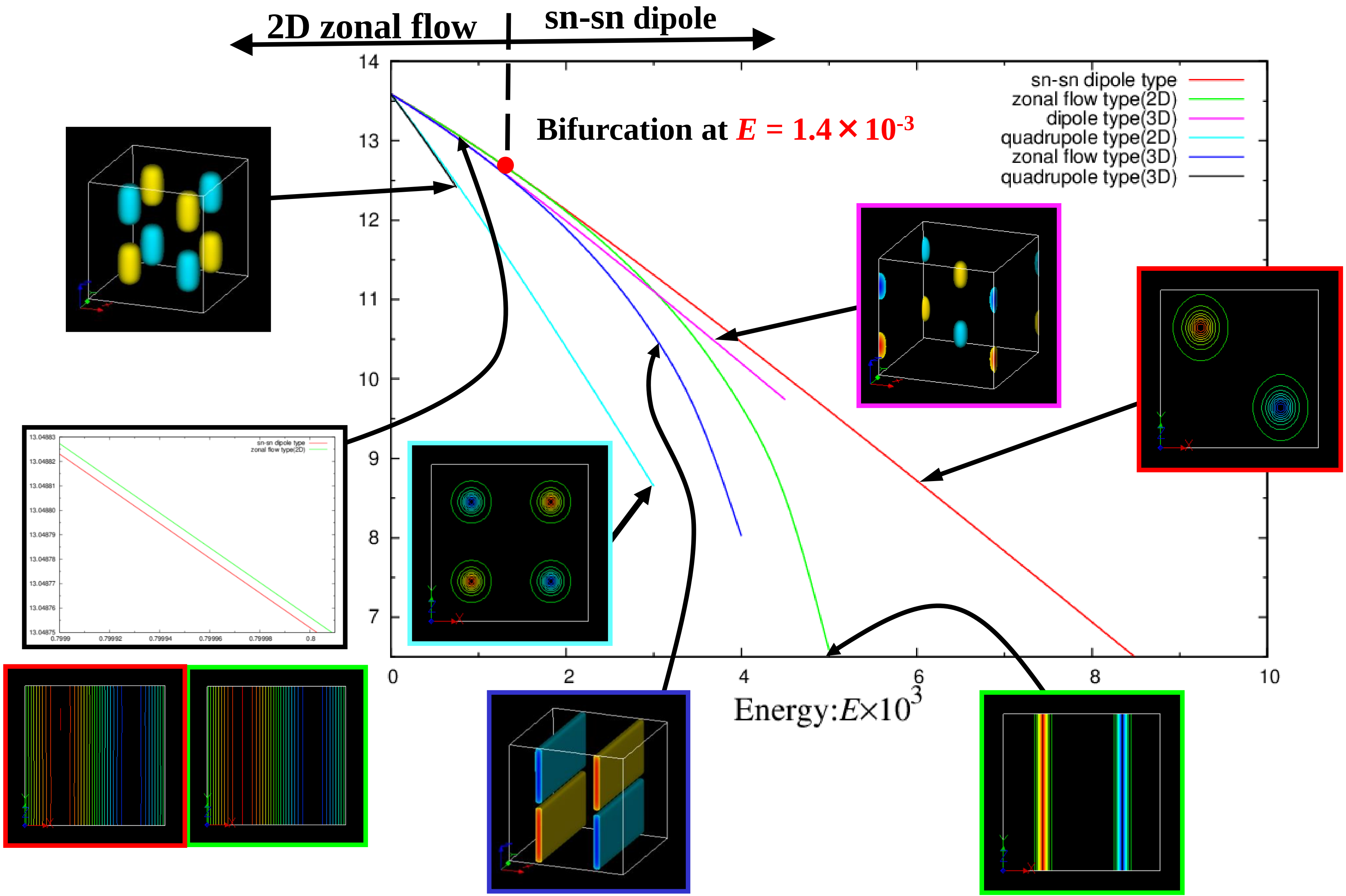

Influence of the Aspect Ratio (1)

Aspect ratio of the periodic domain: $x : y : z = 2\pi : \pi : 2\pi$

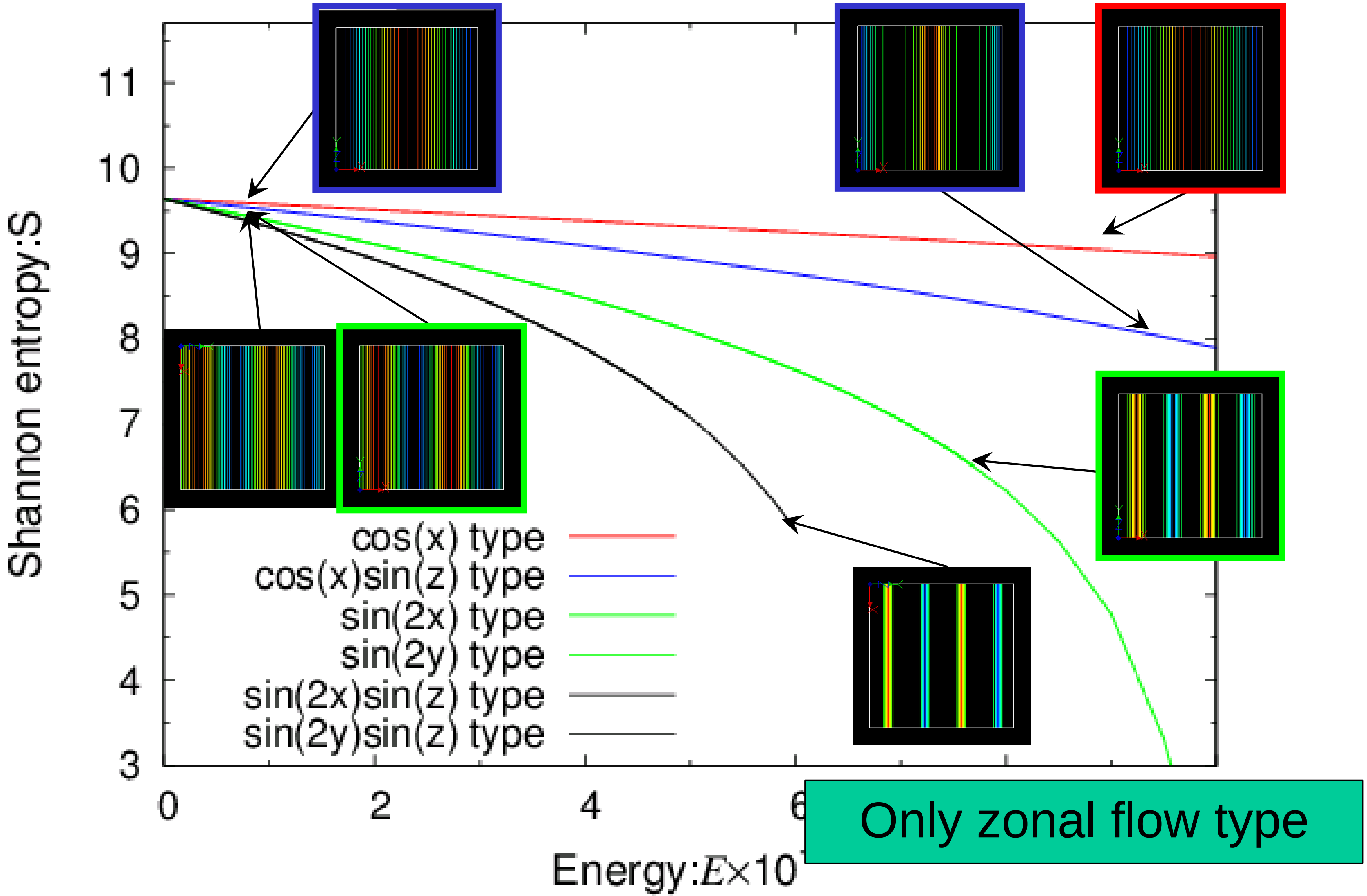

Influence of the Aspect Ratio (2)

Aspect ratio of the periodic domain: $x : y : z = 2\pi : 1.8\pi : 2\pi$

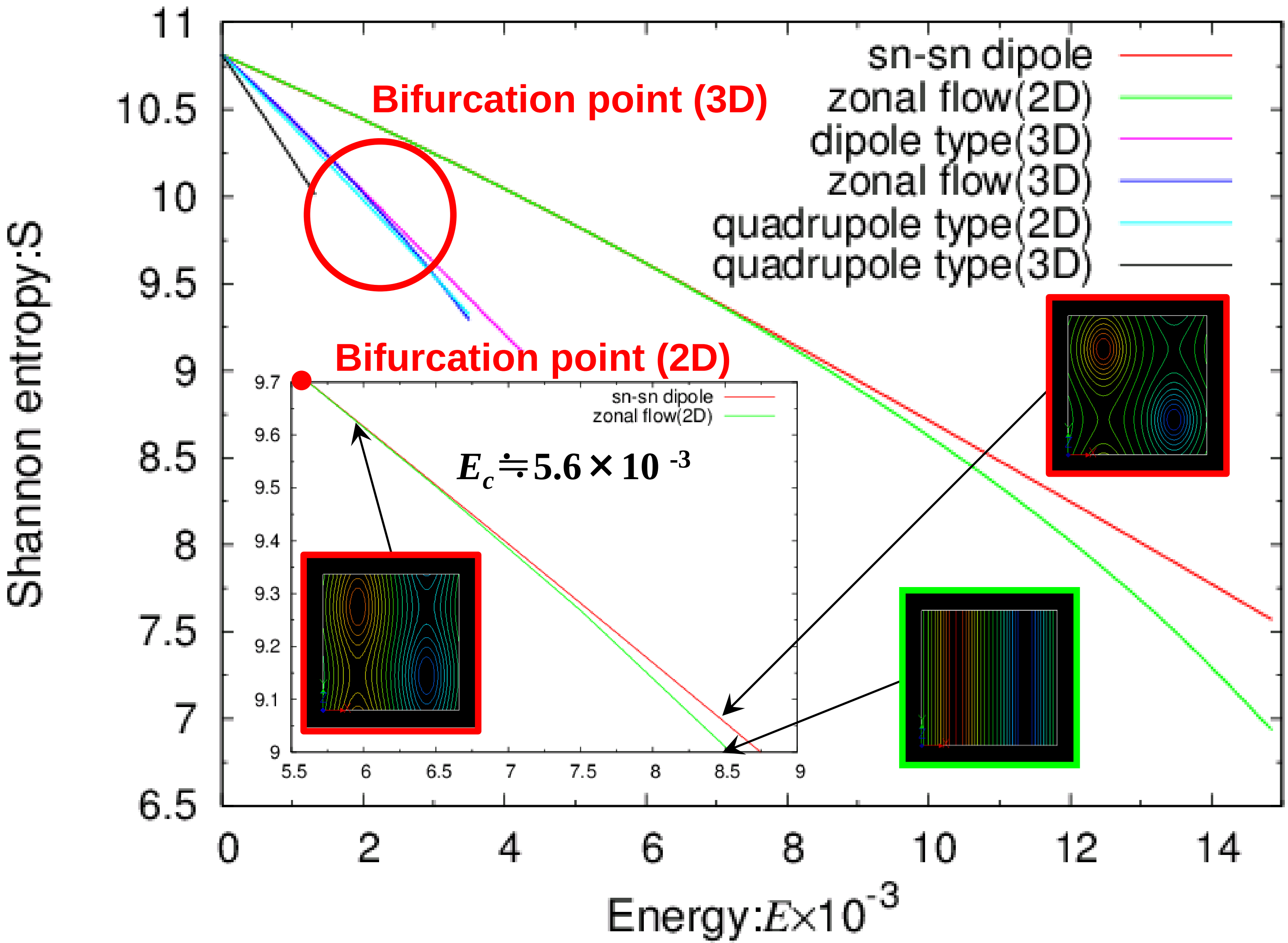

Transition from 3D zonal to 3D dipole type

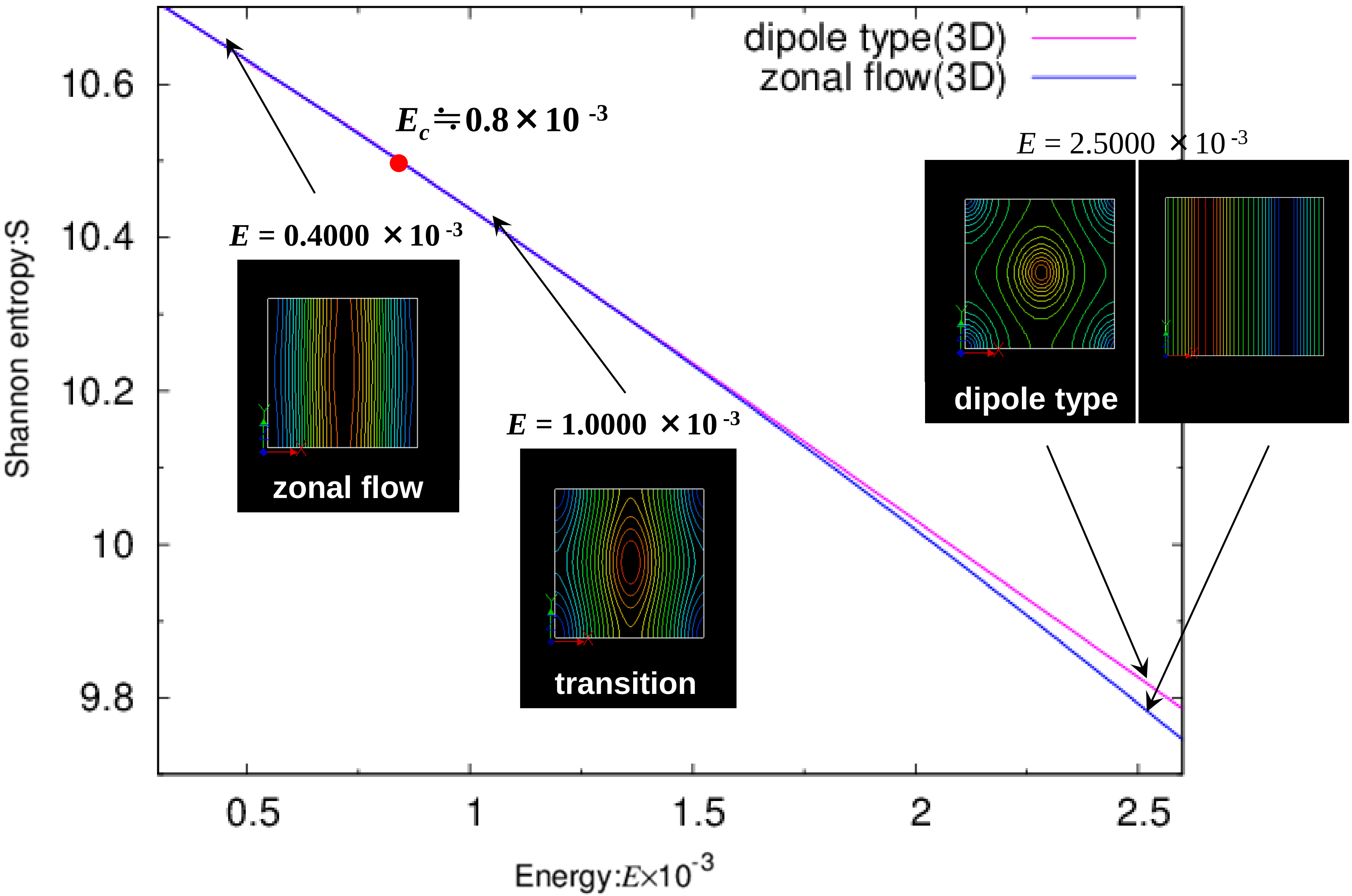

Cluster Strength

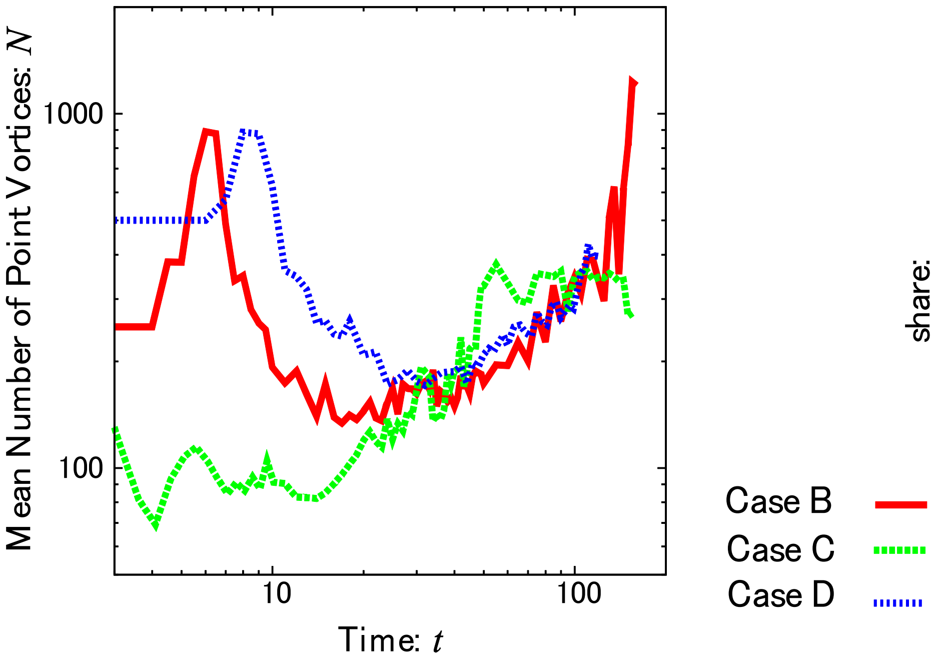

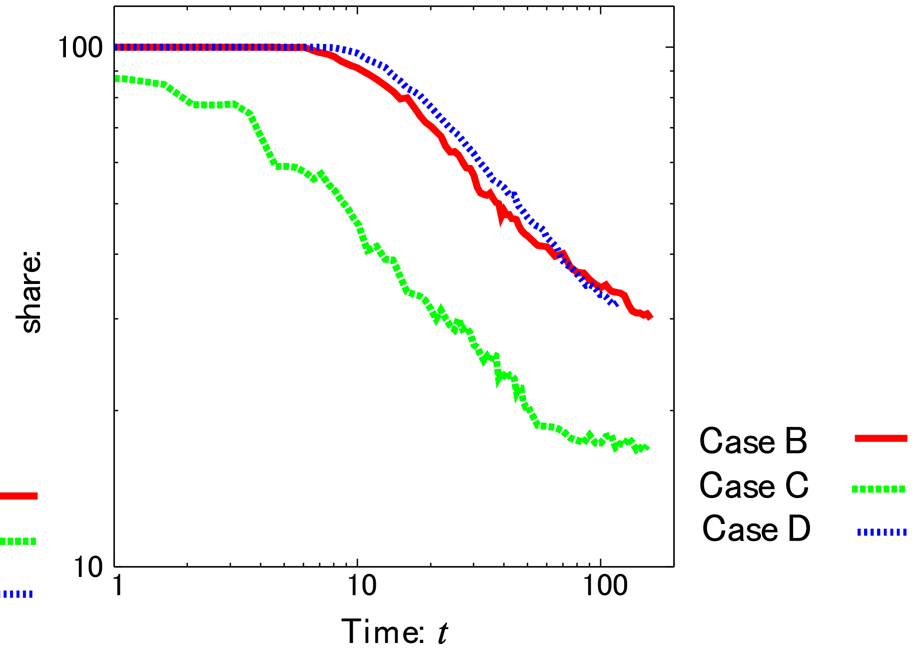

- Number of point vortices in a cluster increases.
- Share of point vortices inside clusters decreases.

- Cluster size grows due to vertical alignment.
- Some of point vortices are emitted from clusters.

スペクトル法による数値計算結果との比較

本研究における
解析結果

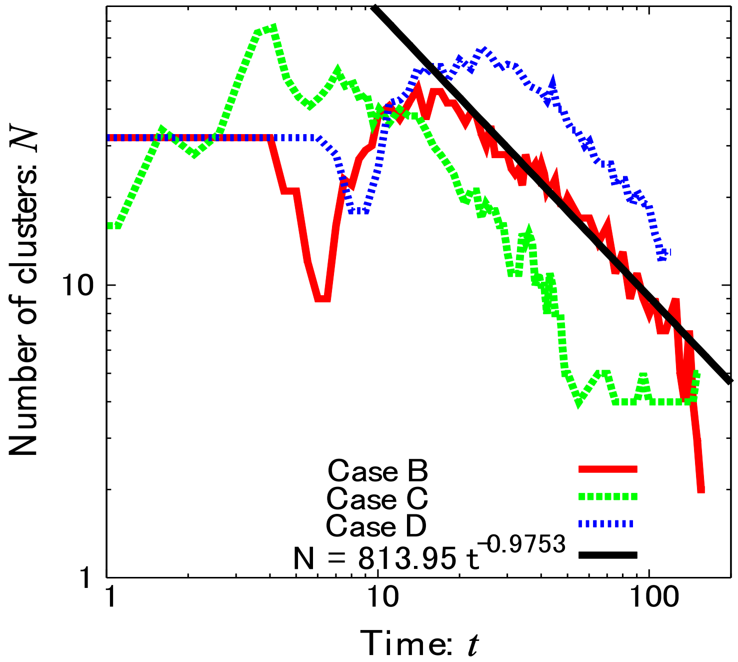

$\sim t^{-1.00}$にしたがってクラスター数が減少

McWilliams *et al.*[2]によるスペクトル法の数値シミュレーション結果

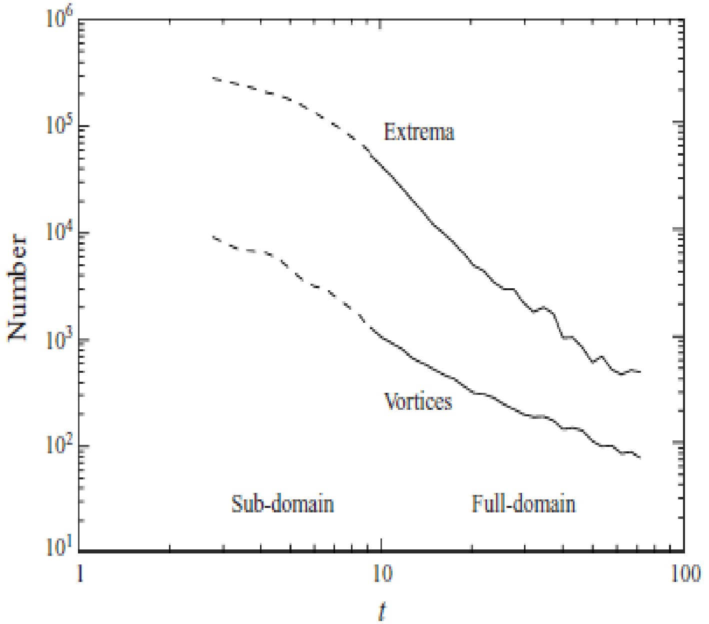

FIGURE 4. The number of extrema and compound vortices, $n_e(t)$ and $n_{cv}(t)$, from the vortex census.

$\sim t^{-1.25}$にしたがって渦数が減少

[2]McWilliams J C, Weiss J B and Yavneh I: *J.Fluid Mech.* **401** 1-16, 1999

スペクトル法による数値計算結果との比較

本研究における解析結果 (Case B)

McWilliams *et al.*[2]によるスペクトル法の数値シミュレーション結果

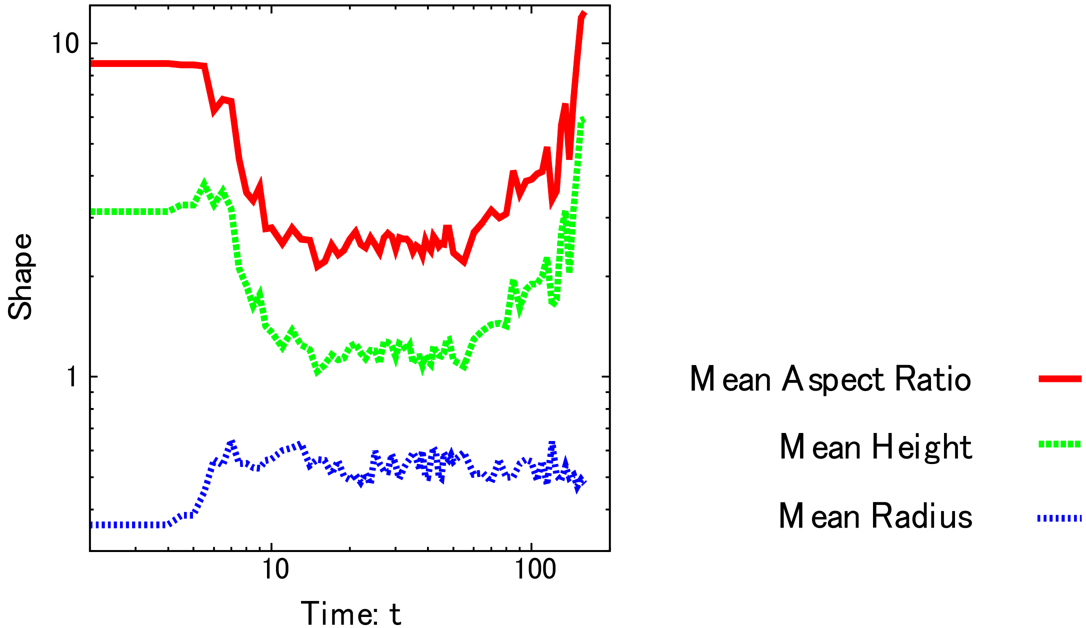

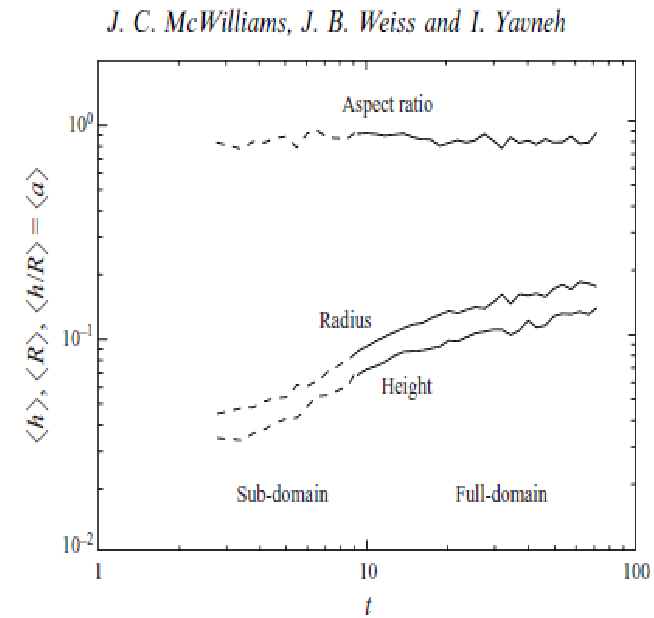

FIGURE 8. The population-mean vortex-element radius, $\langle R \rangle(t)$, half-height, $\langle h \rangle(t)$, and aspect ratio, $\langle a \rangle(t)$, from the vortex census.

- 平均半径がほとんど変化しない
- アスペクト比と高さが同程度のスピードで増加

- 平均半径と平均高さが同程度のスピードで増加
- アスペクト比の変化がほとんどない

[2]McWilliams J C, Weiss J B and Yavneh I: *J.Fluid Mech.* **401** 1-16, 1999

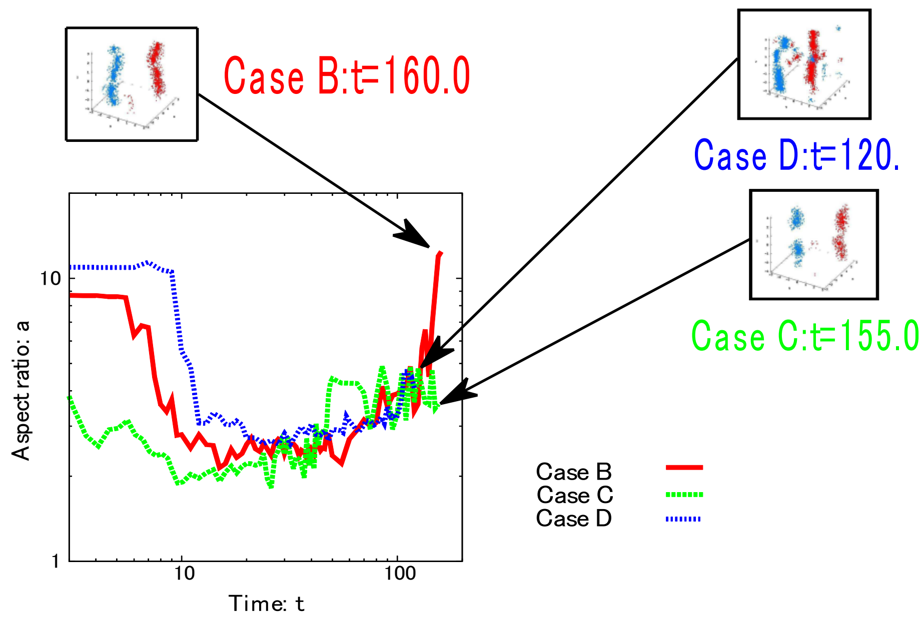
Case B:t=160.0
Case D:t=120.
Case C:t=155.0
10
1
Aspect ratio: a
10
100
Time: t
Case B
Case C
Case D

End States

$L_x : L_y : L_z = 2\pi : 2\pi : 2\pi$

3D view

Top view

Case A: **3D dipole**

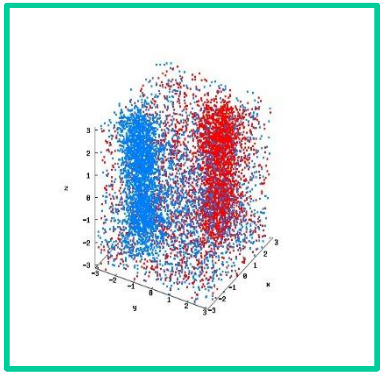

Case B: **Checkerboard**

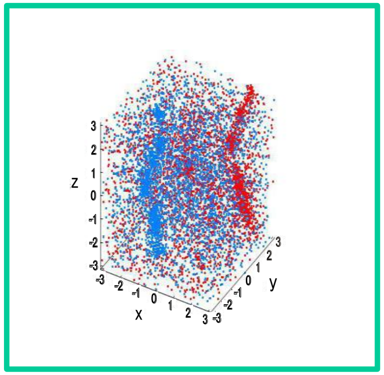

Case A: **3D dipole**

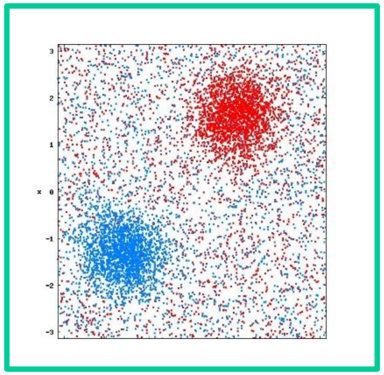

Case B: **Checkerboard**

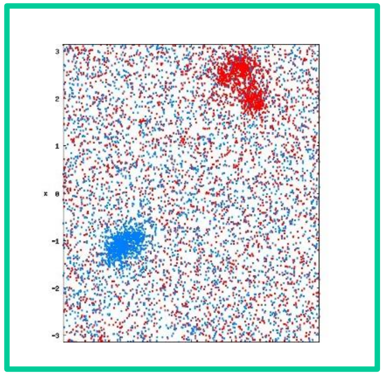

Case C: **16 pillars**

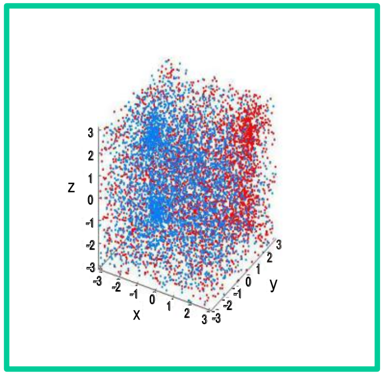

Case D: **Checkerboard**

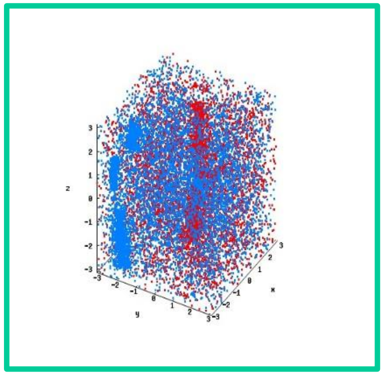

Case C: **16 pillars**

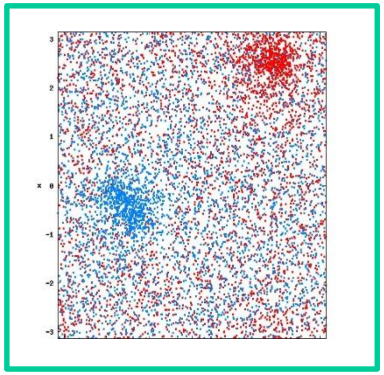

Case D: **Checkerboard**